concentration of conjugated DXR and total dose of drugs were less than at 4 h after administration in both the DXR-conjugate group and DXR-conjugate + HT group. However, the total dose of drugs was still approximately 2-fold higher than baseline at 24 h after administration, and the drug concentration in the tumor was still higher when HT was used (Table IV). These results support the suggestion that HT has an effect on the pharmacokinetics of DXR-conjugate, and the results were similar to those of conventional studies in which HT has been combined with liposomes (31,44). The widening and opening of gaps between endothelial cells may account for the increased tumor drug delivery (31,36,38,39,45). Functional and structural studies have shown that large pores exist in tumor vessels (46). Hyperthermic conditions lead to a rapid reduction and rearrangement of endothelial cell F-actin stress fibres (47,48), which would allow larger pores to be formed between cells (39). If the HT does not exceed 43°C, the change in the endothelium appears to be reversible within 24 h (47). One study in a model of ovarian carcinoma (SKOV-3) showed that 6 h after HT (41°C for 1 h) the degree of extravasation of nanoparticles had returned to baseline (38). Thus the tumor model used, the size of the drug, and the thermal dose affect the results.

*Antitumor efficacy of DXR-conjugate with or without HT.* From the findings of the dose-response relationship after administering 1.25-30 mg/kg of DXR-conjugate (data not shown), the maximum tolerated dose (MTD) of DXR-conjugate in nude mice was estimated to be approximately 40 mg/kg, and one-quarter and one-eighth of the MTD were used in the assessment of antitumor efficacy. The IR increased from 26.2 to 46.1% in the DXR 10 mg/kg group and DXR-conjugate 10 mg/kg group and from 8.0 to 36.2% ($p<0.05$) in the DXR 5 mg/kg group and the DXR-conjugate 5 mg/kg group respectively. Tashiro reported that the MTD of DXR in nude mice is 12 mg/ kg, with an IR of LU99 cells of 28% (22). In the present study the IR of DXR 10 mg/kg was nearly equal to that of DXR at the MTD. Another study has shown that the sensitivity of LU99 to DXR is probably low because of the distribution of DXR in the tumor tissue, which depends on the pH (49,50) and is higher in the range of 6.2-7.6 (50). The results of the present study show that antitumor efficacy was enhanced by using a DDS with a macromolecular carrier (i.e., accumulation of DXR in tumor tissue).

Comparison of the IR in the DXR-conjugate 10 mg/kg group and the DXR-conjugate 10 mg/kg i.v. + HT group showed that it increased from 46.1 to 63.5%, and from 36.2 to 52.0% ($p<0.05$) between the DXR-conjugate 5 mg/kg and DXR-conjugate 5 mg/kg + HT groups. Thus, antitumor efficacy was enhanced to almost the same extent, 16-17 points, in the groups in which HT was used. Because the IR was 13.6% in the group treated with HT alone, we consider that enhancement of the antitumor efficacy of the DXR-conjugate by HT is an additive effect to its own cytocidal effect of HT (Tables III and IV). The evaluation of the toxicity of DXR-conjugate using weight loss as an indicator showed that toxicity tended to be reduced by the combined use of HT. The specific mechanism remains unknown, but one possible reason is that the drug's concentration in the tumor was enhanced and thus the tumor selectivity of the DXR-conjugate was increased by the combined use of HT.

A newly synthesized compound, DXR-conjugate, exerted antitumor efficacy that was significantly superior to that of DXR alone in a nude mouse model. In addition, combined use of DXR-conjugate and HT resulted in an increase in the DXR-conjugate concentration in the tumor, significantly enhancing the drug's antitumor efficacy. Using weight loss as an indicator, toxicity was not increased by the combined use of HT.

## References


1. Lowenthal RM and Eaton K: Toxicity of chemotherapy. Hematol Oncol Clin North Am 10: 967-990, 1996.
2. Matsumura Y and Maeda H: A new concept for macromolecular therapeutic in cancer chemotherapy: mechanism of tumoritropic accumulation of proteins and antitumor agent smancs. Cancer Res 46: 6387-6392, 1975.
3. Maeda H, Wu J, Sawa T, Matsumura Y and Hori K: Tumor vascular permeability and EPR effect in macromolecular theraputics: a review. J Control Release 65: 271-284, 2000.
4. Maeda H: The enhanced permeability and retention (EPR) effect in tumor vascular: the key role of tumor-selective macromolecular dug targeting. Adv Enzyme Regul 41: 189-207, 2001.
5. Dvorak H: Identification and characterization of the blood vessels of solid tumors that are leaky to circulating macromolecules. Am J Pathol 133: 95-109, 1998.
6. Jain R: Extravascular transport in normal and tumor tissue. Crit Rev Oncol Hematol 5: 115-170, 1986.
7. Inoue K: Glyco-technology and DDS. Farumashia 29: 1256-1260, 1993.
8. Nogusa H: Synthesis of carboxymethylpulluan-peptide-doxorubicin conjugates and their properties. Chem Pharm Bull 43: 1931-1938, 1995.
9. Sugawara S: Characteristics of tissue distribution of various polysaccharides as drug carriers: influences of molecular weight and anionic charge on tumor targeting. Biol Pharm Bull 24: 535-543, 2001.
10. Kumazawa E and Ochi Y: DE-310, a novel macromolecular carrier system for the camptotecin analog DX-8951f: potent antitumor activities in various murine tumor models. Cancer Sci 95: 168-175, 2004.
11. Masubuchi N: Pharmacokinetics of DE-310, a novel macromolecular carrier system for the camptothescin analog DX-8951f, in tumor-bearing mice. Pharmazie 59: 374-377, 2004.
12. Engin K: Thermoradiotherapy in the management of superficial malignant tumors. Clin Cancer Res 1: 1139-1145, 1995.
13. Field SB: An Introduction to the Practical Aspects of Clinical Hyperthermia. Taylor and Francis: London, 1990.
14. Dewhirst M, Prosnitz L, Tharll D, *et al*: Hyperthermic treatment of malignant diseases: current status and a view toward the future. Semin Oncol 24: 616-625, 1997.
15. Karino T, Koga S and Maeta M: Experimental studies of the effects of local hyperthermia on blood flow, oxygen pressure and pH in tumors. Jpn J Surg 18: 276-283, 1988.
16. Song CW: Effect of local hyperthermia on blood flow and microenvironment (Review). Cancer Res 44 (suppl 1): S4721-S4730, 1984.
17. Engin K: Biological rationale and clinical experience with hyperthermia. Control Clin Trials 17: 316-342, 1996.
18. Feyerabend T: Rationale and clinical status of local hyperthermia, radiation and chemotherapy in locally advanced malignancies. Anticancer Res 17: 2895-2897, 1997.
19. Issels R: Hyperthermia combined with chemotherapy: biological rationale, clinical application and treatment results. Oncology 22: 374-381, 1999.
20. Matthew CB: Hyperthermia-induced changes in the vascular permeability of rats: a model system to examine therapeutic interventions. J Thermal Biol 25: 381-386, 2000.
21. Inaba M: Evaluation of antitumor activity in a human breast tumor/nude mouse model with a special emphasis on treatment dose. Cancer 64: 1577-1582, 1989.
22. Tashiro T: Responsiveness of human lung cancer/nude mouse to antitumor agents in a model using clinically equivalent doses. Cancer Chemother Pharmacol 24: 187-192, 1989.

23. Hori K, Suzuki M, Tanda S, Saito S and Zhang QH: Functional characterization of developing tumor vascular system and drug delivery (Review). Int J Oncol 2: 289-296, 1993.
24. Ringsdorf H: Structure and properties of pharmacologically active polymers. J Polym Sci Polym Symp 20: 135-153, 1975.
25. Allen TM: Liposomal drug formulations: rationale for development and what we can expect in the future. Drugs 56: 747-756, 1998.
26. Duncan R: Drug-polymer conjugates: potential for improved chemotherapy. Anticancer Drugs 3: 175-210, 1992.
27. Jones M and Leroux J: Polymer micelles - a new generation of colloidal drug carriers. Eur J Pharm Biopharm 48: 101-111, 1999.
28. Langer R: Drug delivery and targeting. Nature 392 (suppl 1): S5-S10, 1998.
29. Massing U: Cancer therapy with liposomal formations of anticancer drugs. Int J Clin Pharm Ther 35: 87-90, 1997.
30. Torchilin VP: Polymer-coated long-circulating microparticulate pharmaceuticals. J Microencapsul 15: 1-19, 1998.
31. Huang SK, Stauffer PR, Hong K, *et al*: Liposomes and hyperthermia in mice: increased tumor uptake and therapeutic efficacy of doxorubicin in sterically stabilized liposomes. Cancer Res 54: 2186-2191, 1994.
32. Kong G and Dewhirst MW: Hyperthermia and liposomes. Int J Hyperthermia 15: 345-370, 1999.
33. Maruyama K, Unezaki S, Takahashi N and Iwastsuru M: Enhanced delivery of doxorubicin to tumor by long-circulating thermosensitive liposomes and local hyperthermia. Biochim Biophys Acta 1149: 209-216, 1993.
34. Unezaki S, Maruyama K, Takahashi N, *et al*: Enhanced delivery and antitumor activity of doxorubicin using long-circulating thermosensitive liposomes containing amphipathic polyethylene glycol in combination with local hyperthermia. Pharm Res 11: 1180-1185, 1994.
35. Fujiwara K and Watanabe T: Effects of hyperthermia radiotherapy and thermoradiotherapy on tumor microvascular permeability. Acta Pathol Jpn 40: 79-84, 1990.
36. Gaber MH, Wu NZ, Hong K, Huang SK, Dewhirst MW and Papahadjopoulos D: Thermosensitive liposomes: extravasation and release of contents in tumor microvascular networks. Int J Radiat Oncol Biol Phys 36: 1177-1187, 1996.
37. Hauck M, Coffin D, Dodge R, Dewhirst MW, Mitchell J and Zalutsky M: A local hyperthermia treatment which enhances antibody uptake in a glioma xenograft model does not affect tumor interstitial fluid pressure. Int J Hyperthermia 13: 307-316, 1997.
38. Kong G, Braun RD and Dewhirst MW: Characterization of the effect of hyperthermia on nanoparticle extravasation from tumor vasculature. Cancer Res 61: 3027-3032, 2001.
39. Lefor A, Makohon S and Ackerman N: The effects of hyperthermia on vascular permeability in experimental liver metastasis. J Surg Oncol 28: 297-300, 1985.
40. Dudar T and Jain R: Differential response of normal and tumor microcirculation to hyperthermia. Cancer Res 44: 605-612, 1984.
41. Eddy HA: Alterations in tumor microvasculature during hyperthermia. Radiology 137: 515-521, 1980.
42. Moriyama E: Cerebral blood flow changes during localized hyperthermia. Neurol Med Chir 30: 923-929, 1990.
43. Nishimura Y, Hiraoka MJS, Akuta K, *et al*: Microangiographic and histologic analysis of the effects of hyperthermia on murine tumor microvasculature. Int J Radiat Oncol Biol Phys 15: 411-420, 1988.
44. Bree VC, Krooshoop JJ, Rietbroek RC, Kipp JBA and Bakker PJM: Hyperthermia enhanced tumor uptake and antitumor efficacy of thermostable liposomes daunorubicin in a rat solid tumor. Cancer Res 56: 563-568, 1996.
45. Clark A, Robins H, Vorpahl J and Yatvin M: Structural changes in murine cancer associated with hyperthermia and lidocaine. Cancer Res 43: 1716-1723, 1983.
46. Yuan F: Transvascular drug delivery in solid tumors. Radiation Oncol 8: 164-175, 1998.
47. Lin PS, Ho KC, Sung SJ and Gladding J: Effect of tumor necrosis factor, heat and radiation on the viability and microfilament organization in cultured endothelial cells. Int J Hyperthermia 8: 667-677, 1992.
48. Ketis NV and Lawler J: Effects of thorobospondin antibody on the recovery of endothelial cells from hyperthermia. J Cell Sci 96: 263-270, 1990.
49. Asaumi J, Kawasaki S, Gao XS, Kuroda M and Hiraki Y: Influence of the extracellular pH, an inhibitor of $Na^+/H^+$ exchanger and an inhibitor of $Cl^-/HCO3^-$ exchanger on adriamycin accumulation. Anticancer Res 15: 71-79, 1995.
50. Asaumi J, Kawasaki S, Nishikawa K, Kuroda M and Hiraki Y: Effects of hyperthermia and cepharanthin on adriamycin accumulation with changes in extracelluar pH. Int J Hyperthermia 11: 27-35, 1995.

*Surgical Techniques*

# Aortic Translocation with Autologous Tissue

**Ryo Aeba, MD**
**Ryohei Yozu, MD**

*Aortic translocation, although technically demanding, could be an excellent surgical option for d-transposition of the great vessels and left ventricular outflow tract obstruction. We report a modification of the aortic translocation technique that uses autologous tissue. The aortic root is mobilized from the right ventricle with an extension of infundibular free-wall muscle for use in closure of the ventricular septal defect, which is similar to the technique for harvesting pulmonary autograft in the Ross-Konno procedure. Our modification may offer an even better surgical outcome for aortic translocation.* ***(Tex Heart Inst J 2007;34:420-2)***

In the surgical management of d-transposition of the great vessels and left ventricular outflow tract (LVOT) obstruction, aortic translocation with biventricular outflow reconstruction may be superior to more conventional repairs such as the Rastelli and LeCompte operations, since the result more closely approximates the normal anatomy. Aortic translocation is accompanied by prosthetic patch repair of the ventricular septal defect (VSD), if the VSD is not too small and restrictive. Avoiding the use of any prosthetic material may offer an even better surgical outcome. We report a technical modification of the aortic translocation technique that uses autologous tissue.

## Case Report

In April 2005, a 3-year-old boy who weighed 15 kg and had significant cyanosis was referred to our hospital for surgical repair of d-transposition, VSD, and LVOT obstruction. He had undergone 2 previous central shunt placements to alleviate severely hypoplastic arborization of the pulmonary artery. Preoperative cardiac evaluation with echocardiography and catheterization showed transposition of the great vessels {S,D,L} and a 1L-2RCx coronary pattern[1] (Fig. 1).

After heart re-exposure and takedown of the previous shunt, we established complete cardiopulmonary bypass with dual venous cannulation and instituted cardiac arrest. Upon opening the right atrium, we noted a conoventricular type of VSD (diameter, 25 mm) with an inlet extension. After division of the ascending aorta a few millimeters distal to the sinotubular junction, we mobilized the aortic root from the right ventricle together with an extension of infundibular free wall muscle, by means of a technique (Fig. 2) similar to pulmonary autograft harvesting in the Ross-Konno procedure. We took care to harvest the aortic root from the right ventricular free wall along a line that would enable a good fit in closing the VSD. The right coronary artery button was removed with a small cuff from the sinus of Valsalva, while the left coronary artery takeoff was left intact to enable aortic root rotation. The defect of the right coronary ostium that was left after harvesting was closed primarily by suture. The LVOT was opened, and the subpulmonic stenotic lesion was resected. The mobilized aortic root was repositioned to the vicinity of the LVOT by means of a 60° counterclockwise rotation. The VSD was closed with the extension cuff of the right ventricular free wall muscle. Next, we performed the LeCompte maneuver, before reattaching the ascending aorta with a rotation and reimplanting the right coronary button. Reconstruction of the right ventricular outflow tract (RVOT) included direct anastomosis of the posterior wall of the pulmonary trunk to the anterior surface of the harvested right ventricular free wall extension. An autologous fresh pericardial patch was used to complete the anterior half of the RVOT.

The patient's postoperative hemodynamic recovery was excellent, and he was doing well 30 months after the operation.

***Key words:*** *Abnormalities, multiple/surgery; aorta/surgery; cardiac surgical procedures; heart ventricles/surgery; transposition of great vessels/surgery*

***From:*** *Division of Cardiovascular Surgery, Keio University, Tokyo 160-8582, Japan*

***Address for reprints:*** *Ryo Aeba, MD, Division of Cardiovascular Surgery, Keio University, 35 Shinanomachi, Shinjuku, Tokyo 160-8582, Japan*

*E-mail: aeba@sc.itc.keio.ac.jp*

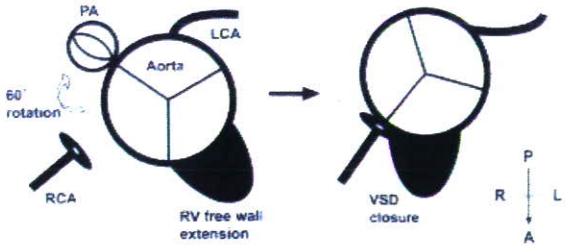


***Fig. 1*** *A cross-sectional drawing shows aortic translocation with use of autologous tissue.*

*A = anterior; L = left; LCA = left coronary artery; P = posterior; PA = pulmonary artery; R = right; RCA = right coronary artery; RV = right ventricle; VSD = ventricular septal defect*

## Discussion

In 1984, Nikaidoh[2] reported an innovative surgical technique in which the entire aortic root is translocated to the posterior of the heart for treating the complex congenital cardiac anomaly present in patients such as ours. Aortic translocation has a potential benefit over more conventional repairs. In a conventional repair, the aortic root is left in the original position, and the rerouted outflow of each ventricle inevitably must make a sharp-angled turn, which may contribute to the suboptimal late outcome that has been reported with this approach.[3] To date, the use of aortic translocation has not been

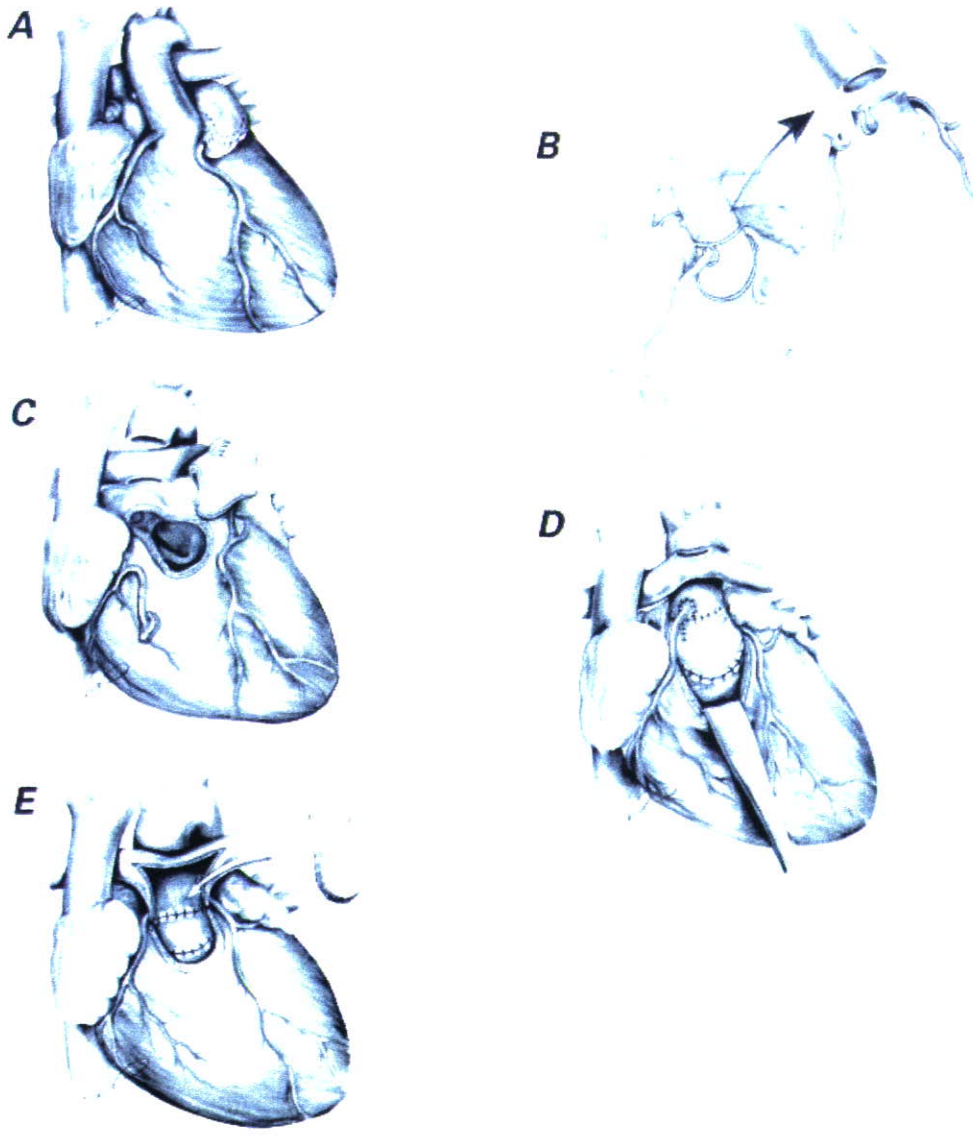


***Fig. 2*** *Schematic representation of the surgical technique of aortic translocation with use of autologous tissue.* ***A****) Appearance of the gross anatomy, with transposition of the great vessels {S,D,L}.* ***B****) The planned incision sites at the aorta, pulmonary trunk, right coronary takeoff, and right ventricular outflow tract.* ***C****) The mobilized aortic root and detached right coronary artery.* ***D****) Aortic translocation with ventricular septal defect closure by means of the right ventricular free wall muscle extension.* ***E****) Reconstruction of the right ventricular outflow tract without the use of a prosthesis.*

widespread, partly because of the highly demanding nature of the procedure and the associated risk of coronary kinking and aortic valve regurgitation. However, several surgeons have recently introduced innovations in the performance of aortic translocation.[4] For example, the ascending aorta may be once divided and re-anastomosed with some rotation, with or without the LeCompte maneuver. One or both of the coronary arteries may be detached from the aortic root and then reimplanted in the appropriate new position if coronary kinking is likely to develop. These surgical procedures are quite analogous to the arterial switch operation.

In our patient, we further modified the technique by using autologous tissue from the harvested aortic root together with an extension of the right ventricular free wall. This manner of harvesting is similar to that used in the Ross-Konno procedure.[5] We determined the optimal location of the most proximal edge of the right ventricular free wall extension by use of a right-angle forceps placed through the ascending aorta and the aortic valve to ensure that the extension would close the VSD, which was previously inspected through a right atriotomy.

Our modification—autologous tissue reconstruction of the LVOT—has several advantages. First, this technique saves 1 suture line between the anterior aortic annulus and the prosthetic patch, therefore simplifying aortic translocation and eliminating a potential site of surgical bleeding and a residual defect. Second, with this technique, the aortic root is free of any suture load when the RVOT is reconstructed, because it has been lowered below the level of the aortic annulus and because the configuration of the aortic sinus of Valsalva is better preserved. Third, when our modification is used, the anterior aortic wall is not tethered, in contrast with aortic translocation performed with VSD patch closure, which tethers the anterior aortic wall and may cause late aortic regurgitation. Lack of a prosthetic patch in the LVOT, which includes the aortic annulus, subjects the aortic annulus to less shear stress and enables the LVOT to grow more uniformly, which might improve the long-term result. Our patient's cardiac anatomy is not uncommon in patients with this anomaly. Therefore, an autologous tissue repair could be used in most cases; patients in whom it would not be appropriate include those with an abnormal coronary artery crossing the right ventricular free wall, a small right ventricular volume, or multiple muscular VSDs.

This report shows that aortic translocation with biventricular outflow reconstruction by means of autologous tissue is technically feasible. Possible advantages over the classic Rastelli, LeCompte, and Nikaidoh procedures need to be demonstrated over time, through the accumulation of surgical experience and long-term follow-up.

## References


1. Gittenberger-de Groot AC, Sauer U, Oppenheimer-Dekker A, Quagebeur JM. Coronary arterial anatomy in transposition of the great arteries: a morphologic study. Pediatr Cardiol 1983;4(Suppl 1):15-24.
2. Nikaidoh H. Aortic translocation and biventricular outflow tract reconstruction. A new surgical repair for transposition of the great arteries associated with ventricular septal defect and pulmonary stenosis. J Thorac Cardiovasc Surg 1984;88:365-72.
3. Kreutzer C, De Vive J, Oppido G, Kreutzer J, Gauvreau K, Freed M, et al. Twenty-five-year experience with Rastelli repair for transposition of the great arteries. J Thorac Cardiovasc Surg 2000;120:211-23.
4. Morell VO, Jacobs JP, Quintessenza JA. Aortic translocation in the management of transposition of the great arteries with ventricular septal defect and pulmonary stenosis: results and follow-up. Ann Thorac Surg 2005;79:2089-93.
5. Reddy VM, Rajasinghe HA, Teitel DF, Haas GS, Hanley FL. Aortoventriculoplasty with the pulmonary autograft: the "Ross-Konno" procedure. J Thorac Cardiovasc Surg 1996; 111:158-67.

EXPERIMENTAL CELL RESEARCH 313 (2007) 2550–2562

available at www.sciencedirect.com

ScienceDirect

www.elsevier.com/locate/yexcr

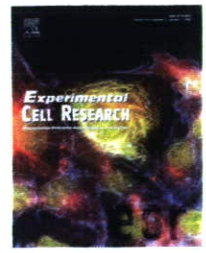

Research Article

# 'Working' cardiomyocytes exhibiting plateau action potentials from human placenta-derived extraembryonic mesodermal cells

Kazuma Okamoto[a,b], Shunichiro Miyoshi[c,d], Masashi Toyoda[a], Naoko Hida[a,c], Yukinori Ikegami[c], Hatsune Makino[a], Nobuhiro Nishiyama[c], Hiroko Tsuji[a,f], Chang-Hao Cui[a], Kaoru Segawa[e], Taro Uyama[a], Daisuke Kami[a], Kenji Miyado[a], Hironori Asada[f], Kenji Matsumoto[g], Hirohisa Saito[g], Yasunori Yoshimura[f], Satoshi Ogawa[c], Ryo Aeba[b], Ryohei Yozu[b], Akihiro Umezawa[a,*]

[a]Department of Reproductive Biology and Pathology, National Research Institute for Child Health and Development, Tokyo, Japan
[b]Department of Surgery, Keio University School of Medicine, Tokyo, Japan
[c]Cardio-pulmonary Division of Keio University School of Medicine, Tokyo, Japan
[d]Institute for Advanced Cardiac Therapeutics, Keio University School of Medicine, Tokyo, Japan
[e]Department of Microbiology and Immunology, Keio University School of Medicine, Tokyo, Japan
[f]Department of Obstetrics and Gynecology, Keio University School of Medicine, Tokyo, Japan
[g]Department of Allergy and Immunology, National Research Institute for Child Health and Development, Tokyo, Japan

ARTICLE INFORMATION

*Article Chronology:*
Received 24 August 2006
Revised version received
19 April 2007
Accepted 24 April 2007
Available online 5 May 2007

*Keywords:*
Placenta
Co-culture
Cardiac differentiation

ABSTRACT

The clinical application of cell transplantation for severe heart failure is a promising strategy to improve impaired cardiac function. Recently, an array of cell types, including bone marrow cells, endothelial progenitors, mesenchymal stem cells, resident cardiac stem cells, and embryonic stem cells, have become important candidates for cell sources for cardiac repair. In the present study, we focused on the placenta as a cell source. Cells from the chorionic plate in the fetal portion of the human placenta were obtained after delivery by the primary culture method, and the cells generated in this study had the Y sex chromosome, indicating that the cells were derived from the fetus. The cells potentially expressed 'working' cardiomyocyte-specific genes such as cardiac myosin heavy chain 7β, atrial myosin light chain, cardiac α-actin by gene chip analysis, and Csx/Nkx2.5, GATA4 by RT-PCR, cardiac troponin-I and connexin 43 by immunohistochemistry. These cells were able to differentiate into cardiomyocytes. Cardiac troponin-I and connexin 43 displayed a discontinuous pattern of localization at intercellular contact sites after cardiomyogenic differentiation, suggesting that the chorionic mesoderm contained a large number of cells with cardiomyogenic potential. The cells began spontaneously beating 3 days after co-cultivation with murine fetal cardiomyocytes and the frequency of beating cells reached a maximum on day 10. The contraction of the cardiomyocytes was rhythmical and synchronous, suggesting the presence of electrical communication between the cells. Placenta-derived human fetal cells may be useful for patients who cannot supply bone marrow cells but want to receive stem cell-based cardiac therapy.



* *Corresponding author.* Fax: +81 3 5494 7048.
E-mail address: umezawa@1985.jukuin.keio.ac.jp (A. Umezawa).

0014-4827/$ – see front matter © 2007 Elsevier Inc. All rights reserved.
doi:10.1016/j.yexcr.2007.04.028

## Introduction

Major advances have been made in the prevention, diagnosis, and treatment of ischemic heart disease and cardiomyopathy, including the use of heart transplantation and artificial hearts. However, the number of patients suffering from heart disease is still increasing [1]. Morbidity and mortality from cardiovascular diseases continue to be an enormous burden experienced by many individuals, with substantial economic cost. Enthusiasm for cell therapy for the injured heart has already reached the clinical setting, with physicians in several countries involved in clinical trials using several types of cell populations [2,3]. Bone-marrow-derived mononuclear cells [4,5], unfractioned bone marrow cells [6], bone-marrow-derived CD133$^+$ cells [7], and myoblasts [8] have been injected into the ischemic heart clinically.

Mesenchymal stem cells (MSCs) are a potential cellular source for stem cell-based therapy, since they have the ability to proliferate and differentiate into mesodermal tissues, including the heart tissue, and entail no ethical problems [9]. Human MSCs have been used clinically to treat patients with graft versus host disease and osteogenesis imperfecta [10,11]. We previously showed that murine and human marrow-derived MSCs can differentiate into cardiomyocytes and start to beat synchronously in vitro [12,13]. In addition, we and other groups proposed that direct injection of murine MSCs into the heart is a feasible approach in murine models of ischemic heart disease and in the normal mouse heart [14,15]. Although MSC transplantation slightly improved impaired cardiac function, this effect was limited. One of the reasons for this may be due to an extremely low rate of cardiomyogenesis from marrow-derived MSCs in vitro [13] and in vivo [14–17]. In order to further improve cardiac function, we have been searching for another source of MSCs having highly cardiomyogenic potential.

The placenta is composed of the amniotic membrane, chorionic mesoderm, and decidua; the amniotic membrane and chorionic mesoderm are the fetal portion and the decidua is the maternal portion (Fig. 1A) [18]. Recently it was reported that the chorionic villi of the placenta differentiated into osteocytes, chondrocytes and adipocytes under specific culture conditions [19,20]. In this study, we generated cells with the mesenchymal phenotype from the chorionic mesoderm, and

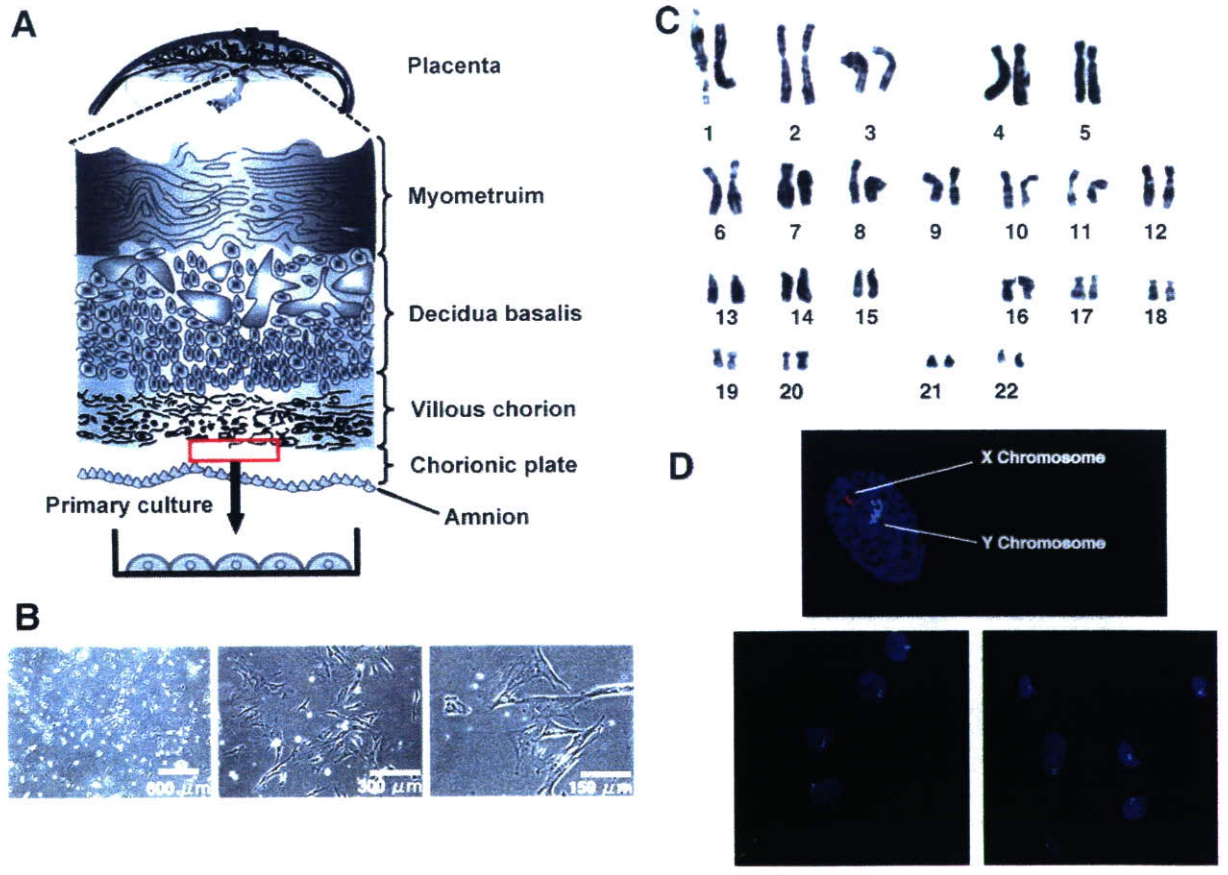


**Fig. 1 – Establishment of chorionic plate cells. (A) Chorionic plate cells were established by primary culture of chorionic plate (red square in the chorionic mesoderm) in the human placenta. (B) Chorionic plate cells at PD 4 consisted of heterogeneous cell population. Three images show chorionic plate cells in the same culture dish. Their shape is different from that of fibroblasts. (C) Karyotyping by G-banding stain of chorionic plate cells. No chromosomal aberration was detected. (D) Chorionic plate cells have one X chromosome (red) and one Y chromosome (light blue). Nuclei were stained with DAPI (blue). (E) Flowcytometric analysis of chorionic plate cells using antibodies for CD14, CD29, CD31, CD34, CD44, CD45, CD59, CD73, CD90, CD105 and CD166. Black lines and shaded areas indicate reactivity of antibodies for isotype controls and that of antibodies for cell surface markers, respectively.**

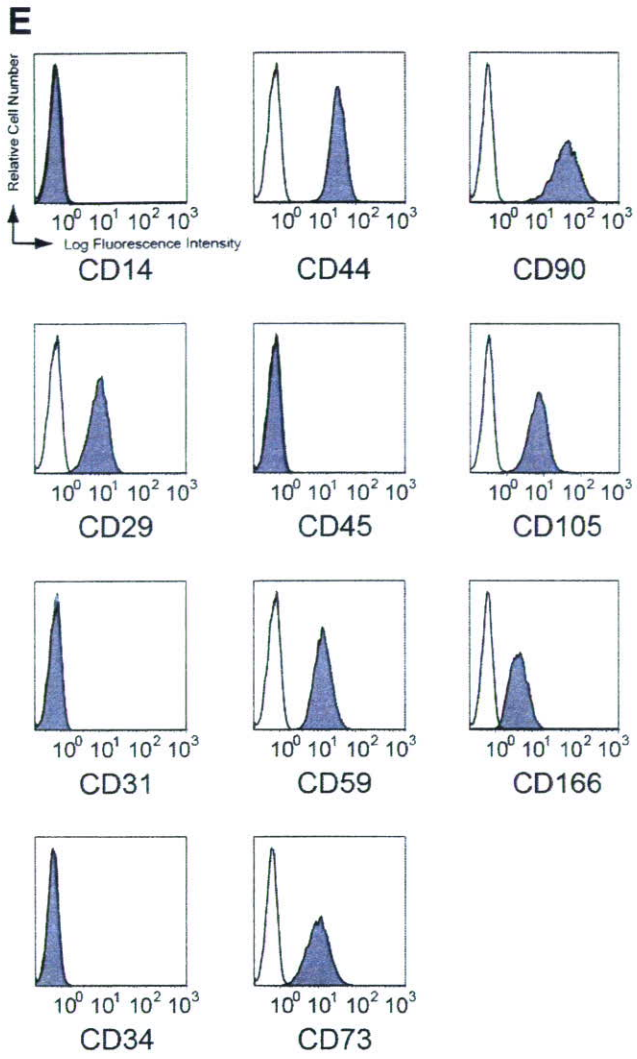


**Fig. 1 (*continued*).**

showed that: (a) physiologically functioning cardiomyocytes were transdifferentiated from human placenta-derived chorionic plate cells, but clear osteogenic and adipogenic phenotypes were not induced; (b) the cardiomyogenic induction rate obtained using our system was relatively high compared to that obtained using the previously described method [13]; (c) co-cultivation with fetal murine cardiomyocytes alone without transdifferentiation factors such as 5-azaC or oxytocin is sufficient for cardiomyogenesis in our system; (d) chorionic plate cells have the electrophysiological properties of 'working' cardiomyocytes. The chorionic mesoderm contained a large number of cells with a cardiomyogenic potential.

## Materials and methods

### *Chorionic plate cell culture*

A human placenta was collected after delivery of a male neonate with informed consent. The study was approved by the ethics committee of Keio University, Tokyo, Japan (Number 17-44-1). To isolate chorionic plate cells, we used the explant culture method, in which the cells were outgrown from pieces of chorionic plate attached to dishes (Fig. 1A). Briefly, the decidua of the maternal part was separated and discarded. The chorionic plate from the fetal part were cut into pieces approximately 5 $mm^3$ in size. The pieces were washed in DMEM (high glucose; Kohjin Bio) supplemented with 100 U/ml penicillin–streptomycin (Gibco), 1 μg/ml Amphotericin B (Gibco) and 4 U/ml Novo-Heparin Injection 1000 (Mochidaseiyaku Co., Ltd.), until the supernatant was free of erythrocytes. Some pieces of chorionic plate were attached to the substratum in a 10-cm-diameter dish (Falcon, Becton, Dickinson and Company (BD), San Jose, CA, USA). Culture medium consisting of DMEM (high glucose; Kohjin Bio) supplemented with 10% FBS (CCT, Cansera, Canada) was added. The cells migrated out from the cut ends after approximately 20 days of incubation at 37 °C in 5% $CO_2$. The migrated cells were harvested with phosphate-buffered saline (PBS) with 0.1% trypsin and 0.25 mM EDTA (ethylenediamine-*N*,*N*,*N*',*N*'-tetraacetic acid) (Immuno-Biological Laboratories) for 5 min at 37 °C and counted. The harvested cells were re-seeded at a density of $3 \times 10^5$ cells in a 10-cm-diameter dish. Confluent monolayers of cells were subcultured at a 1:8 split ratio onto new 10-cm-diameter dishes and designated "chorionic plate cells". The culture medium was replaced with fresh culture medium every 3 or 4 days. The chorionic plate cells used in this study were within five to nine population doublings (approximately two to five passages).

### *Reverse transcriptase (RT)-PCR*

Chorionic plate cells at PD 6 were dissociated with 0.1% trypsin and 0.25 mM EDTA for 5 min at 37 °C. Total RNA was extracted with RNeasy (Qiagen). Human cardiac RNA was purchased (Clontech). RNA for RT-PCR was converted to cDNA with Superscript (Invitrogen) according to the manufacturer's recommendations. RT-PCR was performed by using primers for the genes of cardiac transcription factors: Csx/Nkx-2.5, GATA4; a cardiac hormone: atrial natriuretic peptide (ANP), brain natriuretic peptide (BNP); cardiac structural proteins: cardiac troponin-I (cTnI), cardiac troponin T (cTnT), myosin light chain-2α (MLC-2α), cardiac actin; and 18s rRNA. 18s rRNA (18S) was used as an internal control. PCR was performed with recombinant Taq (Toyobo Co., Ltd.) or TaKaRa LA Taq with GC Buffer (Takara Shuzo Co., Ltd.) for 30 or 35 cycles, with each cycle consisting of 95 °C for 30 s, 55 °C, 61 °C or 65 °C for 45 s, and 2 °C for 45 s, with an additional 5-min incubation at 72 °C after completion of the final cycle. The PCR was performed in 50 μl of buffer (10 mmol/l Tris–HCl (pH 8.3), 2.5 mmol/l $MgCl_2$, and 50 mmol/l KCl) containing 1 mmol/l each of dATP, dCTP, dGTP, and dTTP, 2.5 U of Gene Taq (Nippon Gene), and 0.2 mol/l primers. The PCR products were size fractionated by 2% agarose gel electrophoresis.

### *Karyotyping of chorionic plate cells*

Metaphase spreads were prepared from chorionic plate cells treated with 100 ng/ml colcemid (Karyo Max, Gibco Co. BRL) for 6 h. We performed karyotyping by G-banding stain on at least 30 metaphase spreads for each population. The CEP X/Y DNA Probe Kit (Vysis) was used to determine the proportion of XX and XY cells in accordance with the manufacturer's suggestions.

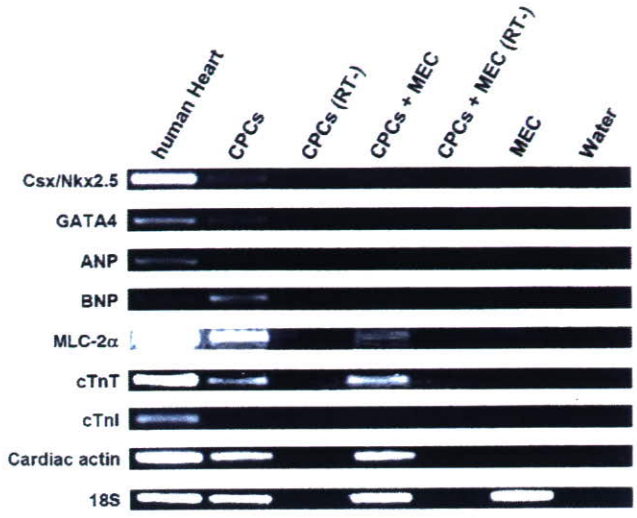


**Fig. 2 – Gene expression of cardiomyocyte-specific/associated genes in chorionic plate cells. RT-PCR analysis revealed expression patterns of cardiomyocyte-specific or associated genes; *Csx/Nkx2.5, GATA4, ANP, BNP, cTnI, cTnT, cardiac actin* and *MLC-2α* (from left to right) in human heart, chorionic plate cells (CPCs), chorionic plate cells after co-culturing with murine embryonic cardiomyocytes (CPCs + MEC), murine embryonic cardiomyocytes (MEC) and water. "RT-" represented an omission of a reverse transcriptase treatment to RNA as negative control. Human heart RNA and water (without RNA) served as positive and negative control, respectively. 18s rRNA (18S) was amplified in parallel reactions as a housekeeping gene serving as an internal control.**

### *Flow cytometric analysis*

Chorionic plate cells were stained for 1 h at 4 °C with primary antibodies and immunofluorescent secondary antibodies. The cells were then analyzed on a Cytomics FC 500 (Beckman Coulter, Inc.) and the data were analyzed with the FlowJo Ver.7 (Tree Star, Inc.). Antibodies against human CD14 (6603511, Beckman Coulter), CD29 (Integrin-β1) (6604105, Beckman Coulter), CD31 (PECAM-1) (IM1431, Beckman Coulter), CD34 (IM1250, Beckman Coulter), CD44 (IM1219, Beckman Coulter, IM1219), CD45 (556828, Beckman Coulter), CD59 (IM3457, Beckman Coulter), CD73 (550257, BD Pharmingen), CD90 (Thy-1) (555596, BD Pharmingen), CD105 (Endoglin) (A07414, Beckman Coulter) and CD166 (ALCAM) (559263, BD Pharmingen) were adopted as primary antibodies.

### *Gene chip analysis*

Human genomewide gene expression was examined with the Human Genome U133A Probe array (Affymetrix), which contains the oligonucleotide probe set for approximately 23,000 full-length genes and expressed sequence tags (ESTs). Total cellular RNA was immediately isolated with the RNeasy (Qiagen), according to the manufacture's instructions. Contaminating DNA was eliminated by DNase I (Takara Bio Inc.). The purity of RNA was assessed on the basis of the A260/A280 ratio, and the integrity of RNA was verified by agarose gel electrophoresis. Double-stranded cDNA was synthesized from DNase-treated total RNA, and the cDNA was subjected to in vitro transcription in the presence of biotinylated nucleoside triphosphates, according to the manufacturer's protocol (One-Cycle Target Labeling and Control Reagent package [http://www.affymetrix.com/support/technical/manual/expression_manual.affx]). The biotinylated cRNA was hybridized with a probe array for 16 h at 45 °C, and the hybridized biotinylated cRNA was stained with streptavidin-PE and scanned with a Hewlett-Packard Gene Array Scanner (Palo Alto). The fluorescence intensity of each probe was quantified by using the GeneChip Analysis Suite 5.0 computer program (Affymetrix). The expression level of a single mRNA was determined as the average fluorescence intensity among the intensities obtained with 11 paired (perfectly matched and single-nucleotide-mismatched) probes consisting of 25-mer oligonucleotides. If the intensities of mismatched probes were very high, gene expression was judged to be absent, even if high average fluorescence was obtained with the GeneChip Analysis Suite 5.0 program. The level of gene expression was determined with the GeneChip software as the average difference (AD). Specific AD levels were then calculated as the percentage of the mean AD level of six probe sets for housekeeping genes (*actin* and *GAPDH* [glyceraldehyde-3-phosphate dehydrogenase] genes). Further data analysis was performed with Genespring software version 5 (Silicon Genetics). To normalize the staining intensity variations among chips, the AD values for all genes on a given chip were divided by the median of all measurements on that chip. To eliminate changes within the range of background noise and to select the most differentially expressed genes, data were used only if the raw data values were less than 100 AD and gene expression was judged to be present by the Affymetrix data analysis.

**Table 1 – RT-PCR primers used in this study**

| | Primer (sense) | Primer (anti-sense) | Annealing temperature (°C) | Product size (bp) |
|---|---|---|---|---|
| Csx/Nkx-2.5 | CTTCAAGCCAGAGGCCTACG | CCGCCTCTGTCTTCTCCAGC | 61 | 233 |
| GATA4 | GACGGGTCACTATCTGTGCAAC | AGACATCGGCACTGACTGAGAAC | 61 | 475 |
| ANP | GAACCAGAGGGGAGAGACAGAG | CCCTCAGCTTGCTTTTTAGGAG | 55 | 406 |
| BNP | CATTTGCAGGGCAAACTGTC | CATCTTCCTCCCAAAGCAGC | 55 | 206 |
| MLC-2α | GAAGGTGAGTGTCCCAGAGG | ACAGAGTTTATTGAGGTGCCCC | 65 | 376 |
| cTnT | GGCAGCGGAAGAGGATGCTGAA | GAGGCACCAAGTTGGGCATGAACGA | 65 | 152 |
| cTnI | CCCTGCACCAGCCCCAATCAGA | CGAAGCCCAGCCCGGTCAACT | 65 | 233 |
| Cardiac actin | CTTCCGCTGTCCTGAGACAC | CCTGACTGGAAGGTAGATGG | 61 | 400 |
| 18S | GTGGAGCGATTTGTCTGGTT | CGCTGAGCCAGTCAGTGTAG | 55 | 200 |

**Table 2 – Human cardiomyocyte-specific or -associated gene expression profiling of undifferentiated and differentiated chorionic plate cells (CPCs)**

| Systematic | Common | Undifferentiated CPCs | | Differentiated CPCs | | Human heart | Description |
|---|---|---|---|---|---|---|---|
| 207317_s_at | CASQ2 | 34 | A | 12 | A | P | Calsequestrin 2 (cardiac muscle) |
| 205553_s_at | CSRP3 | 8 | A | 5 | A | P | Cysteine and glycine-rich protein 3 (cardiac LIM protein) |
| 208040_s_at | MYBPC3 | 56 | A | 117 | A | P | Myosin binding protein C, cardiac |
| 214468_at | MYH6 | 11 | A | 50 | A | P | Myosin, heavy polypeptide 6, cardiac muscle, alpha (cardiomyopathy, hypertrophic 1) |
| 204737_s_at | MYH7 | 5 | A | 161 | P | P | Myosin, heavy polypeptide 7, cardiac muscle, beta |
| 216265_x_at | MYH7 | 36 | A | 232 | A | P | Myosin, heavy polypeptide 7, cardiac muscle, beta |
| 215795_at | MYH7B | 89 | A | 11 | A | P | Myosin, heavy polypeptide 7B, cardiac muscle, beta |
| 209742_s_at | MYL2 | 267 | A | 153 | A | P | Myosin, light polypeptide 2, regulatory, cardiac, slow |
| 210088_x_at | MYL4 | 338 | P | 404 | A | P | Myosin, light polypeptide 4, alkali; atrial, embryonic |
| 210395_x_at | MYL4 | 220 | P | 412 | P | P | Myosin, light polypeptide 4, alkali; atrial, embryonic |
| 219942_at | MYL7 | 9 | A | 16 | A | P | Myosin, light polypeptide 7, regulatory |
| 207557_s_at | RYR2 | 11 | A | 13 | A | P | Ryanodine receptor 2 (cardiac) |
| 214044_at | RYR2 | 17 | A | 23 | A | P | Ryanodine receptor 2 (cardiac) |
| 205742_at | TNNI3 | 96 | A | 195 | A | P | Troponin I, cardiac |
| 215389_s_at | TNNT2 | 83 | A | 165 | A | P | Troponin T2, cardiac |
| 205132_at | ACTC | 289 | P | 671 | P | P | Actin, alpha, cardiac muscle |
| 206029_at | ANKRD1 | 214 | P | 13 | A | P | Ankyrin repeat domain 1 (cardiac muscle) |
| 213738_s_at | ATP5A1 | 5905 | P | 2657 | P | P | ATP synthase, $H^+$ transporting, mitochondrial F1 complex, alpha subunit, isoform 1, cardiac muscle |
| 205444_at | ATP2A1 | 107 | A | 53 | A | A | ATPase, $Ca^{++}$ transporting, cardiac muscle, fast twitch 1 |
| 209186_at | ATP2A2(SERCA2A) | 4465 | P | 2577 | P | P | ATPase, $Ca^{++}$ transporting, cardiac muscle, slow twitch 2 |
| 212361_s_at | ATP2A2(SERCA2A) | 814 | P | 338 | A | P | ATPase, $Ca^{++}$ transporting, cardiac muscle, slow twitch 2 |
| 212362_at | ATP2A2(SERCA2A) | 178 | P | 60 | A | A | ATPase, $Ca^{++}$ transporting, cardiac muscle, slow twitch 2 |
| 207317_s_at | CASQ2 | 34 | A | 12 | A | P | Calsequestrin 2 (cardiac muscle) |
| 65472_at | | 6 | A | 17 | A | A | qb80a04.x1 Soares_fetal_heart_NbHH19W *Homo Sapiens* cDNA clone IMAGE:1706382 3′ similar to TR:O21123 O21123 CYTOCHROME OXIDASE I; mRNA sequence |
| 205298_s_at | BTN2A2 | 482 | P | 183 | A | A | zd240d07.s1 Soares_fetal_heart_NbHH19W *Homo sapiens* cDNA clone IMAGE:341581 3′, mRNA sequence |
| 213121_at | SNRP70 | 66 | A | 6 | A | A | zd39c08.s1 Soares_fetal_heart_NbHH19W *Homo sapiens* cDNA clone IMAGE:343022 3′, mRNA sequence |
| 65521_at | LOC51619 | 658 | A | 266 | A | P | zd56g04.r1 Soares_fetal_heart_NbHH19W *Homo sapiens* cDNA clone IMAGE:344694 5′, mRNA sequence |

| | | | | | | | |
|---|---|---|---|---|---|---|---|
| 214014_at | CDC42EP2 | 38 | A | 14 | A | A | zd85d03.s1 Soares_fetal_heart_NbHH19W *Homo sapiens* cDNA clone IMAGE:347429 3', mRNA sequence |
| 201204_s_at | RRBP1 | 2174 | P | 1257 | P | P | zf44f12.s1 Soares_fetal_heart_NbHH19W *Homo sapiens* cDNA clone IMAGE:379823 3', mRNA sequence |
| 209331_s_at | MAX | 561 | P | 294 | P | P | zg72g05.s1 Soares_fetal_heart_NbHH19W *Homo sapiens* cDNA clone IMAGE:398936 3', mRNA sequence |
| 214776_x_at | XYLB | 24 | A | 13 | A | A | zi99g02.s1 Soares_fetal_liver_spleen_1NFLS_S1 *Homo sapiens* cDNA clone IMAGE:448946 3', mRNA sequence |
| 211715_s_at | BDH | 59 | A | 8 | A | P | 3-hydroxybutyrate dehydrogenase (heart, mitochondrial) |
| 205534_at | PCDH7 | 8 | A | 205 | P | A | BH-protocadherin (brain–heart) |
| 205535_s_at | PCDH7 | 7 | A | 75 | P | P | BH-protocadherin (brain–heart) |
| 210273_at | PCDH7 | 157 | A | 168 | A | P | BH-protocadherin (brain–heart) |
| 210941_at | PCDH7 | 14 | A | 3 | A | A | BH-protocadherin (brain–heart) |
| 204726_at | CDH13 | 172 | P | 195 | P | P | Cadherin 13, H-cadherin (heart) |
| 203020_at | HHL | 210 | P | 117 | P | P | Expressed in hematopoietic cells, heart, liver |
| 213982_s_at | HHL | 335 | P | 74 | P | P | Expressed in hematopoietic cells, heart, liver |
| 205738_s_at | FABP3 | 79 | A | 92 | P | P | Fatty acid binding protein 3, muscle and heart (mammary-derived growth inhibitor) |
| 214285_at | FABP3 | 22 | A | 49 | A | P | Fatty acid binding protein 3, muscle and heart (mammary-derived growth inhibitor) |
| 220138_at | HAND1 | 246 | A | 117 | A | P | Heart and neural crest derivatives expressed 1 |
| 220480_at | HAND2 | 19 | A | 29 | A | A | Heart and neural crest derivatives expressed 2 |
| 213036_x_at | ATP2A3 | 23 | A | 25 | A | A | *Homo sapiens* SERCA3 gene, exons 1–7 (and joined CDS) |
| 204938_s_at | PLN | 22 | A | 60 | A | P | Phospholamban |
| 204939_s_at | PLN | 71 | A | 99 | A | P | Phospholamban |
| 204940_at | PLN | 46 | A | 28 | A | P | Phospholamban |
| 206578_at | NKX2-5 | 40 | A | 14 | A | P | NK2 transcription factor related, locus 5 (*Drosophila*) |
| 205517_at | GATA4 | 16 | A | 46 | A | P | GATA binding protein 4 |
| 201667_at | GJA1 | 4792 | P | 2016 | P | P | Gap junction protein, alpha 1, 43 kDa (connexin 43) |
| 208636_at | ACTN1 | 7896 | P | 3182 | P | P | Actinin, alpha 1 |
| 208637_x_at | ACTN1 | 5400 | P | 2359 | P | P | Actinin, alpha 1 |
| 211160_x_at | ACTN1 | 5727 | P | 1529 | P | A | Actinin, alpha 1 |
| 203861_s_at | ACTN2 | 38 | A | 17 | A | P | Actinin, alpha 2 |
| 203862_s_at | ACTN2 | 53 | A | 16 | A | P | Actinin, alpha 2 |
| 203863_at | ACTN2 | 35 | A | 20 | A | P | Actinin, alpha 2 |
| 203864_s_at | ACTN2 | 189 | A | 123 | A | P | Actinin, alpha 2 |
| 206891_at | ACTN3 | 134 | M | 133 | A | M | Actinin, alpha 3 |
| 200601_at | ACTN4 | 1134 | P | 282 | P | P | Human non-muscle alpha-actinin mRNA, complete cds |
| 211805_s_at | SLCBA1(NCX1) | 53 | A | 228 | A | P | Solute carrier family 8 (sodium/calcium exchanger), member 1 |
| 207413_s_at | SCN5A | 32 | A | 61 | A | P | Sodium channel, voltage-gated, type V, alpha (long QT syndrome 3) |

### *Introduction of the EGFP gene*

Recombinant adenovirus carrying the enhanced green fluorescent protein (EGFP) gene was prepared as described [13]. Chorionic plate cells were plated on dishes at $2\times10^5/cm^2$, and infected with EGFP-expressing adenovirus at 10 plaque-forming units/cell on the next day. Chorionic plate cells were examined in vitro by fluorescent confocal microscopy for expression of the EGFP gene. By 7 days post-infection, nearly all of the cells expressed EGFP. To eliminate the possibility of free adenovirus in the cell supernatant, we infected murine fetal cardiomyocytes with chorionic plate cell supernatants after infection. No murine fetal cardiomyocytes expressed EGFP, implying that the cells are not transfected with free adenovirus.

### *Preparation of murine fetal cardiomyocytes*

Fetal cardiomyocytes were obtained from the hearts of day 17 mouse fetuses. The hearts were minced with scissors and washed with PBS, and then incubated in PBS with 0.1% trypsin and 0.25 mM EDTA for 10 min at 37 °C. After DMEM supplemented with 10% FBS was added, the cardiomyocytes were centrifuged at 1000 rpm for 5 min. The pellet was then re-suspended in 10 ml of DMEM with 10% FBS and incubated on glass dishes for 1 h to separate the cardiomyocytes from fibroblasts. The floating cardiomyocytes were collected and re-plated at $5\times10^4/cm^2$.

### *Co-culture system of chorionic plate cells and murine fetal cardiomyocytes*

Neither 5-azaC [12] nor oxytocin [21] was used in this process as they are known to initiate cardiomyogenic differentiation. EGFP-labeled chorionic plate cells were harvested with 0.25% trypsin and 1 mM EDTA and overlaid onto the cultured fetal cardiomyocytes at $7\times10^3/cm^2$. Every 2 days the culture medium was replaced with fresh culture medium that was supplemented with 10% FBS and 1 μg/ml Amphotericin B (Gibco). The morphology of the beating EGFP-labeled chorionic plate cells was evaluated under a fluorescent microscope. The image was monitored using a CCD camera and stored as digital video. The cell contraction was analyzed using an image-edge detection program made by Igor Pro 4 (Wavemetrics Inc., Lake Oswego, Oregon).

### *Electrophysiological analysis*

On day 10 of co-cultivation, action potentials (APs) were recorded as described previously [12,13] from spontaneously beating EGFP-labeled cells. Spontaneously beating EGFP-positive chorionic plate cells were selected as targets. The APs of the targeted cells had been recorded and Alexa568 dye was injected by iontophoresis to confirm that the APs were generated by EGFP-positive chorionic plate cells. The extent of dye transfer was monitored under a fluorescence microscope, and digital images were recorded with a digital photo camera (D100; Nikon, Tokyo, Japan) mounted on a microscope with a fluorescence filter (UMWIG2; Olympus).

### *Immunocytochemistry*

A laser confocal microscope (LSM510, Zeiss) was used for immunocytochemical analysis. The chorionic plate cells co-cultured with fetal cardiomyocytes in vitro were fixed with 2% paraformaldehyde (PFA) in PBS for 20 min at 4 °C and treated with 0.1% Triton-X PBS for 20 min at room temperature. These cells were then stained with mouse monoclonal anti-human cardiac troponin-I antibody (#4T21/19-C7 HyTest, Euro, Finland) diluted 1:300, monoclonal anti-α-actinin antibody (Sigma) diluted 1:300, and anti-connexin 43 antibody (Sigma) diluted 1:300. To prevent fading and to stain nuclei, a Slow Fade Light Antifade kit with 4′-6-diamidino-2-phenylindole (DAPI) (Molecular Probes) was used.

## Results

### *Establishment of chorionic plate cells*

Almost all human tissues or organs can be a source of MSCs, which have been extracted from fat, muscle, menstrual blood, endometrium, placenta, umbilical cord, cord blood, skin, and eye. In this study, we focused on cells derived from fetuses, since fetus-derived cells tend to both differentiate and proliferate better than adult cells [22]. In that sense, human placenta is a good source of fetus-derived MSCs. We cultivated chorionic plate cells that were obtained from the chorionic mesoderm of the placenta (Fig. 1A). The chorionic plate cells regarded as being Population Doubling (PD) 0 or Day 0 were fibroblast-like in morphology, indistinguishable in appearance from the marrow-derived MSCs, and relatively larger in size than rapidly self-renewing stem cells [23] (Fig. 1B). The cells from PD 9 to PD 18 rapidly proliferated in culture and were propagated continuously. Chorionic plate cells did not undergo malignant transformation. They stopped dividing after reaching confluence and they did not form any foci after reaching confluence in vitro.

To clarify the character of the established chorionic plate cells, we first performed karyotypic analysis of 30 cells at PD 3. All cells had normal chromosomes without any chromosomal aberration (Fig. 1C). The sex chromosomes were found to be XY, implying that all cells were of fetal origin. Genomic FISH analysis also revealed that all cells had XY chromosomes (Fig. 1D). We examined the cell surface marker of the placenta-derived cells (chorionic plate cells) by FACS analysis (Fig. 1E). The surface markers of chorionic plate cells are exactly the same as those of previously reported bone-marrow- and cord blood-derived mesodermal cells, i.e., positive for CD29, CD44,

**Fig. 3 – Immunocytochemistry of chorionic plate cells for human cardiac troponin-I. (A–F) Immunocytochemistry of differentiated chorionic plate cells with anti-human cardiac troponin-I (cTnI) antibody. The EGFP-positive cells (B) were stained with anti-human cTnI antibody (A) and the merged image (DAPI, EGFP, cTnI) is shown in panels D and F. An enlarged image (red square in D) is shown in panel E. Clear striations were observed with red fluorescence of cTnI in the differentiated cells. (G–I) A merged image for EGFP and cTnI is shown in panel G. A longitudinal section at the green line in the merged image G is shown in panel H. An axial section at the red line in merged image G is shown in panel I.**

CD59, CD73, CD 90, CD105 and CD166, and negative for CD14, CD31, CD34 and CD45.

Next we investigated whether chorionic plate cells have cardiomyogenic potential by human cardiomyocyte-specific gene expression using RT-PCR method (Fig. 2, Table 1) and gene chip analysis (Table 2; GEO accession number, GSE7021: GSM162104 and GSM162105). Chorionic plate cells expressed Csx/Nkx-2.5, GATA4, BNP, cardiac troponin T (cTnT), cardiac

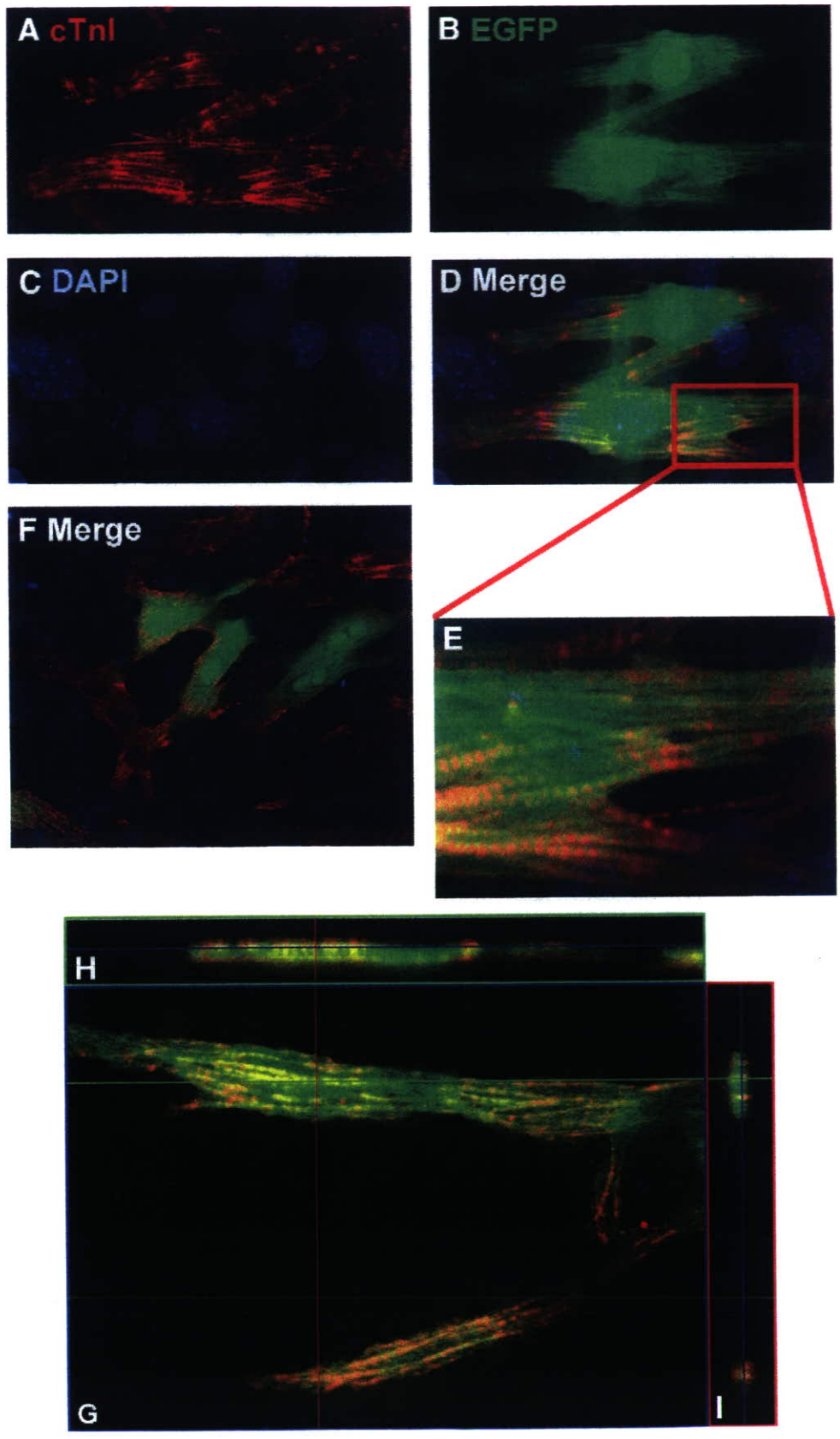

actin and myosin light chain-2α (MLC-2α) in the default state, implying that chorionic plate cells can differentiate into cardiomyocytes, like CMG cells in which Csx/Nkx-2.5 and GATA4 are constitutively expressed before induction [12].

### *Cardiomyogenic differentiation of chorionic plate cells*

employed a co-culture system with murine fetal cardiomyocytes to induce cardiac differentiation, since in vitro simulation of the heart by the environment has been shown to be an efficient means of inducing the differentiation of human endothelial progenitor cells [15] and human marrow stromal cells [13]. EGFP-labeled chorionic plate cells were co-cultured with murine fetal cardiomyocytes without any chemical treatment. A few EGFP-positive chorionic plate cells started to contract on day 3 after the start of co-cultivation, and beat strongly and rigorously in a synchronized manner on day 5 (Supplementary movie 1). The cells continued to beat at least until day 21 during the period of observation. The frequency of cardiomyogenic differentiation from chorionic plate cells was calculated based on the number of cTnI-positive cells. In three independent experiments, the percentage of cells that underwent cardiomyogenic differentiation was similar (15.1±5.1%) (Supplementary Fig. 1S). Our investigation of the cardiomyogenic-specific gene expression for differentiated chorionic plate cells (Fig. 2) found that cardiac actin was fully expressed, whereas Csx/Nkx-2.5 and cardiac troponin T were only slightly expressed. GATA4, cTnI, MLC-2α, and BNP were not expressed. Technical difficulties may have adversely affected these results, as some of the differentiated cells divided from murine fetal cardiomyocytes were physically damaged and so the ratio of differentiated to undifferentiated cells may well have been diminished in each case. In fact, in every experiment, cTnI was detected by immunocytochemical analysis. Immunocytochemical staining revealed that EGFP-labeled cells stained positive for cTnI (Figs. 3A–F). Immunostaining of longitudinal sagittal and axial transverse sections confirmed that cTnI was expressed in the EGFP-positive cells (Figs. 3G–I, Supplementary movie 2). These results imply that co-culture system of chorionic plate cells and murine embryonic cardiomyocytes induces differentiation of chorionic plate cells into cTnI-positive cells in vitro. cTnI-positive cells were evenly detected throughout the dish, suggesting that the cardiomyogenic induction rate was quite high in the present model. The EGFP-positive cells also expressed α-actinin, and connexin 43 (Figs. 4A–E). Clear striations were observed for the red fluorescence of cTnI (Fig. 3A) and α-actinin (Fig. 4A) in the differentiated chorionic plate cells. Connexin 43 staining (Figs. 4C–G) showed a clear and diffuse pattern around the margin of the cytoplasm, suggesting that these human transdifferentiated cardiomyocytes have tight electrical coupling with each other. We also performed in vivo implantation of EGFP-labeled chorionic plate donor cells into the ischemic heart model of nude rats (data not shown). EGFP-labeled chorionic plate donor cells exhibit positive cTnI reactivities at the implanted site. However, the frequency of cTnI-positive cells in vivo is not comparative with that in vitro.

To investigate if chorionic plate cells are capable of differentiating into osteoblasts and adipocytes [19,20], we induced chorionic to differentiate into osteocytes and adipocytes under specific culture conditions. Chorionic plate cells did not show clear adipogenic and osteogenic differentiation: cells did not accumulate Oil Red O-positive fat droplets and calcium, and did not increase alkaline phosphatase osteogenic activity (Supplementary Fig. 2S), suggesting that chorionic plate cells have a cardiomyocyte potential, but not adipocyte or osteoblast potential.

### *The action potential of differentiated chorionic plate cells*

To detect the electrophysiological coupling due to gap-junctional communication between beating cardiomyocytes, action potentials (APs) were recorded from spontaneously beating EGFP-positive cells. Alexa568 was injected into cells via a recording microelectrode to stain the cells and to confirm that the APs were generated by EGFP-positive cells (Figs. 5A–C). The dye did not diffuse into the murine cardiomyocytes, indicating that there were no tight cell-to-cell heterologous connections, i.e., gap junctions. Alexa568 dye did not diffuse into adjacent human and murine cells of the injected cells that exhibited action potentials. The action potentials obtained originate from human chorionic plate cells or may result from electrical coupling with adjacent cardiomyocytes [24]. The APs obtained from chorionic plate cells showed clear cardiomyocyte-specific sustained plateaux (Figs. 5D, E) and were therefore concluded to be APs of cardiomyocytes, not of smooth muscle cells, nerve cells, or skeletal muscle cells. The measured parameters of the recorded AP were averaged (Fig. 5F). Chorionic plate cells had the character of 'working' cardiomyocytes or ordinary cardiomyocytes. The rhythm of almost all the beating cells had become regular at 1 week. The fractional shortening (%FS) of the cells was analyzed (Supplementary Fig. 3S), using a cell-edge detection program developed by S.M. The EGFP-positive cells contracted simultaneously within the whole visual field, suggesting tight electrical communication among them. The average %FS was 5.46±0.40% ($n=10$). In summary, human cardiomyocytes obtained from the chorionic plate cells were electrophysiologically and physiologically functional.

## Discussion

### *Transdifferentiation of human extraembryonic mesodermal cells into embryonic mesodermal cells: functional working cardiomyocytes*

This study was conducted to determine whether extensive ex vivo propagation by cell culture would prevent the cardiomyogenic differentiation of placenta-derived cells. According to our previous study on the induction of cardiomyogenic differentiation of immortalized murine marrow stromal cells [12,15] and human marrow stromal cells [13] by demethylating agents, the transdifferentiation of human stromal cells was limited to working cardiomyocytes and did not include pacemaker cells. This was probably due to the origin of cells, that is, the default state of the chorionic plate-derived human fetal cells used in the experiment. The idea for the cardiomyogenic differentiation protocol using murine fetal cardiomyocytes without 5-azacytidine arose from reports that endothelial cells differentiate into cardiomyocytes as a result of co-cultivation with murine fetal cardiomyocytes [25].

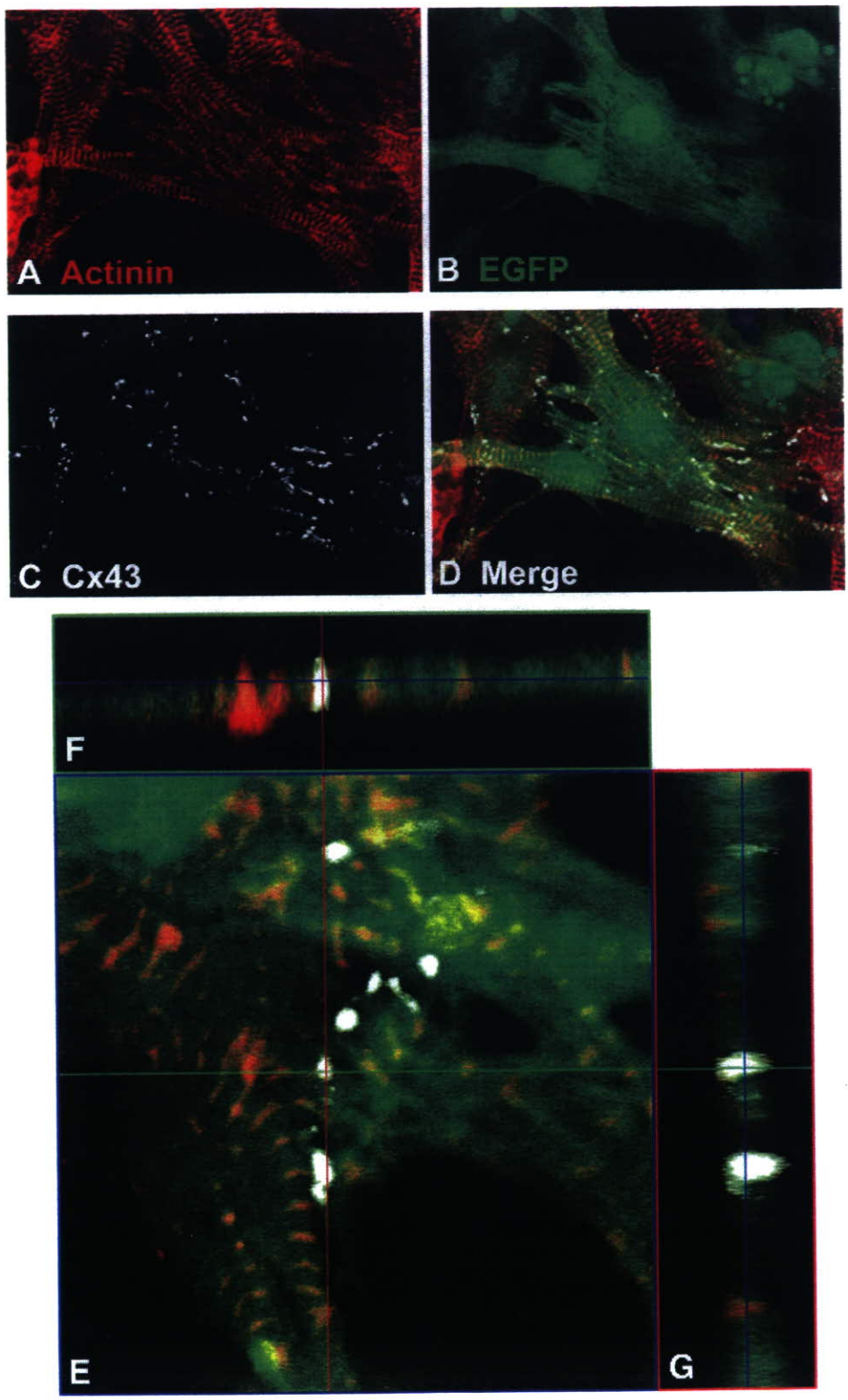


Fig. 4 – Immunocytochemistry of chorionic plate cells for α-actinin and connexin 43. (A–D) Immunocytochemistry of differentiated chorionic plate cells for α-actinin (Actinin) and connexin 43 (Cx43) antibody. Clear striations were observed for the red fluorescence of α-actinin (A) in the EGFP-positive cells (B). Connexin 43 (C) was stained along the attachment site of EGFP-positive cells. Merged images (α-actinin, connexin 43, EGFP) are shown in panel D. (E–G) A merged image for α-actinin, connexin 43, and EGFP is shown in panel E. (F) A longitudinal section at the green line in merged image E. (G) An axial section at the red line in merged image E. Panels F and G show that connexin 43 is located between EGFP-positive cells.

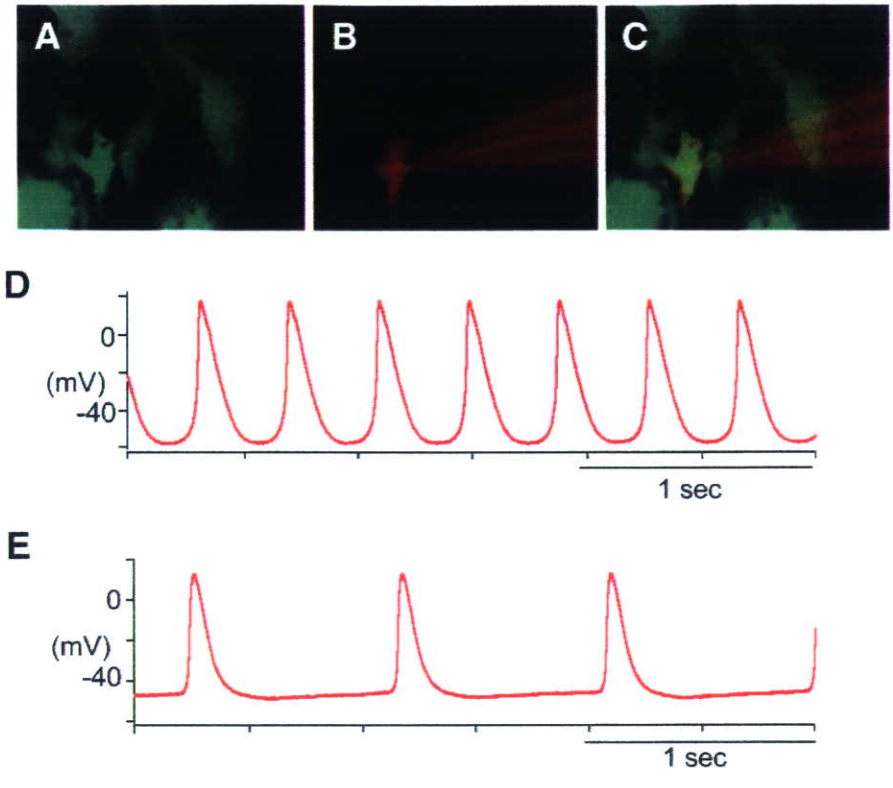


F

| | Amplitude (mV) | Resting Membrane Potential (mV) | APD90 (msec) | APD50 (msec) | RR (sec) | Vmax (V/s) | n |
|---|---|---|---|---|---|---|---|
| PLKC | 63.87± 2.24 | -52.22± 1.05 | 209.1± 12.9 | 100.2± 4.8 | 0.948± 0.138 | 4.460± 0.355 | 14 |

**Fig. 5 – Electrophysiological and physiological analysis of chorionic plate cells. (A–C) EGFP-labeled chorionic plate cells were injected with Alexa568 solution by ionophoresis through a microelectrode. (D, E) Two different types of action potential, i.e., tachycardia type and bradycardia type, were recorded. Both types of cells had the features of working cardiomyocytes. The rhythm of their beating was regular. (F) The measured action potential parameters of EGFP-labeled chorionic plate cells are averaged.**

The high frequency of cardiomyogenic differentiation makes it inconceivable that the transdifferentiation is due to fusion; in addition, bone marrow stromal cells [13] do not fuse with feeder cells in the co-cultivation system and the frequency of fusion in the co-culture system is not high [26] in contrast to myogenic differentiation [27]. The global gene expression pattern showed that the change in gene expression during differentiation was consistent with phenotypic alteration. The cells established from the placenta can be extensively and clonally expanded in vitro while retaining their potential to differentiate into cardiomyocytes that exhibit spontaneous beating and cardiomyocyte-specific action potential under in vitro conditions. This differentiation potential shown by the placenta-derived cells is the same as that reported for bone marrow MSCs [12,13,15]. It is also noteworthy that the transdifferentiation of chorionic plate cells represents the transition from extraembryonic cells to embryonic cells, while the transdifferentiation from bone-marrow-derived MSCs to neurogenic cells, which we previously reported [28,29], is transition between germ layers in embryonic tissues.

Most of the surface markers of the placenta-derived cells examined in this study are the same as those detected in their bone marrow counterparts [13,30], with both cord blood- and bone-marrow-derived mesodermal cells being positive for CD29, CD44, and CD59, and negative for CD34. Our finding of in vitro differentiation from extraembryonic mesodermal cells to embryonic mesodermal cells in this study, a key future goal for any cell-based therapy, could thus be achieved by exposing placenta-derived cells to murine fetal cardiomyocytes, at least in vitro. This technique allows the applications of the placenta to be further extended and permits it to be used as an alternative to bone marrow as a source of cells with cardiomyogenic potential.

### *Is the high rate of cardiomyogenic differentiation of placenta-derived cells due to the default cell state?*

The cardiomyogenic differentiation rate of chorionic plate cells (15.1%) was relatively high compared to that of marrow-derived MSCs (less than 0.3%) [13]. The gene expression

pattern of chorionic plate cells before cardiomyogenic differentiation was different from that of marrow-derived MSCs. The expression of cardiomyocyte-associated genes in the chorionic plate cells, which we unexpectedly found by GeneChip analysis and confirmed by RT-PCR, is surprising. Constitutive expression of the Csx/Nkx2.5 cardiogenic 'master' gene [31,32] in the chorionic plate cells with the ability of self-renewal suggests that the chorionic plate cells have cardiogenic potential [33] and may be termed "cardiac precursor cells" in the light of their biological characteristics like endometrium-derived myogenic procursor cells [27]. The mechanism of the drastic improvement in the differentiation rate of chorionic plate cells may be attributable to default characteristics as cardiac precursor cells of the placenta-derived cells in culture. Because of this improvement in the differentiation rate, it is possible to obtain a large number of cardiomyocytes without prolongation of their life span, i.e., transfer of oncogenic molecules into cells, to restore cardiac function. It is quite interesting that working cardiomyocytes can be generated from placenta-derived cells, since one of the types of target cells for regenerative medicine is heart cells.

### *Are human placenta-derived cells that are propagated in vitro useful for cell-based therapy?*

Can primary placenta-derived cell 'culture' contribute to cell-based therapy or regenerative medicine? Primary placenta-derived cell culture obtained from the chorionic mesodermal layer succeeded in almost 100% of the attempts, and the cells were passaged only 3 or 4 times (6 to 7 PDs) before reaching premature senescence. The problems involved in cell-based therapy with human placenta-derived cells are the finite life span of the cells and the difficulty of obtaining a large enough number of cells. Based on the results of our previous study using cord blood-derived cells, the establishment of cells can be explained by: (1), lack of $p16^{INK4a}$ in primary-cultured cells, or (2), selection of cells that do not express $p16^{INK4a}$ from a heterogeneous population [22]. We cannot exclude either possibility, and we did observe two different types of cells, i.e., rapidly growing spindle cells and quiescent flat and elongated cells in the primary culture of placenta cells. Experimental settings that allow human placenta cells to double more than 100 times may be used to obtain a large number of cells at least from the placenta.

We believe that these placenta-derived extraembryonic mesodermal cells may be used to supply cardiomyocytes to patients with ischemic heart disease, dilated cardiomyopathy, and Kawasaki disease, which all have a poor prognosis and are sometimes lethal. The 'risk versus benefit' balance is essential when applying these multiplied cells clinically and the 'risk' or 'drawback' in this case is the transformation of implanted cells. In vivo experiments revealed that no tumor was observed for up to 4 weeks when chorionic plate cells at P5 ($1\times10^7$) were subcutaneously inoculated into immunodeficient, non-obese diabetic (NOD)/severe combined immunodeficiency (SCID)/interleukin 2 $receptor^{-/-}$ (NOG) mice (data not shown). Human placenta-derived cells spontaneously avoid premature senescence without gene induction and enter replicative senescence. Replicative senescence may be due to a tumor suppressor mechanism that avoids the risk of cell transformation after implantation of cells as a source for cell-based therapy [34].

Our present study suggested the presence of a precursor cell type in the placenta which is destined to generate 'working cardiomyocytes'. Since the placenta is usually discarded, it can be collected at usual delivery or cesarean section and can be banked or stored. Cells with almost all the HLA types can be collected after several generations. A placenta-derived cell bank system covering all HLA types may be necessary for patients who cannot supply bone marrow cells but want to receive stem cell-based cardiac therapy.

## Acknowledgments

We would like to express our sincere thanks to A. Crump for critically reading the manuscript, A. Oka and M. Terai for the support throughout the work, and K. Saito for the secretarial work. This study was supported by grants from the Ministry of Education, Culture, Sports, Science and Technology (MEXT) of Japan; by the Suntory Fund for Advanced Cardiac Therapeutics, Keio University School of Medicine; Health and Labor Sciences Research Grants, and the Pharmaceuticals and Medical Devices Agency; by the Research on Health Science Focusing on Drug Innovation from the Japan Health Science Foundation; by the Program for Promotion of Fundamental Studies in Health Science of the Pharmaceuticals and Medical Devices Agency (PMDA); by a research Grant for Cardiovascular Disease from the Ministry of Health, Labor and Welfare; by a Grant for Child Health and Development from the Ministry of Health, Labor and Welfare; and by a grant from Terumo Life Science Foundation. A part of the work was done at the Pfizer Keio Research Laboratory Center for Integrated Medical Research.

Data set from the gene chip analysis are available at the GEO database with accession number GSE7021: GSM162104 and GSM162105.

## Appendix A. Supplementary data

Supplementary data associated with this article can be found, in the online version, at doi:10.1016/j.yexcr.2007.04.028.

## REFERENCES

[1] T. Thom, N. Haase, W. Rosamond, V.J. Howard, J. Rumsfeld, T. Manolio, Z.J. Zheng, K. Flegal, C. O'Donnell, S. Kittner, D. Lloyd-Jones, D.C. Goff Jr., Y. Hong, R. Adams, G. Friday, K. Furie, P. Gorelick, B. Kissela, J. Marler, J. Meigs, V. Roger, S. Sidney, P. Sorlie, J. Steinberger, S. Wasserthiel-Smoller, M. Wilson, P. Wolf, Heart disease and stroke statistics—2006 update: a report from the American Heart Association Statistics Committee and Stroke Statistics Subcommittee, Circulation 113 (2006) e85–e151.

[2] A. Leri, J. Kajstura, P. Anversa, Cardiac stem cells and mechanisms of myocardial regeneration, Physiol. Rev. 85 (2005) 1373–1416.

[3] M.A. Laflamme, C.E. Murry, Regenerating the heart, Nat. Biotechnol. 23 (2005) 845–856.

[4] H.F. Tse, Y.L. Kwong, J.K. Chan, G. Lo, C.L. Ho, C.P. Lau, Angiogenesis in ischaemic myocardium by intramyocardial autologous bone marrow mononuclear cell implantation, Lancet 361 (2003) 47–49.
[5] E. Perin, Transendocardial injection of autologous mononuclear bone marrow cells in end-stage ischemic heart failure patients: one-year follow-up, Int. J. Cardiol. 95 (Suppl 1) (2004) S45–S46.
[6] K.C. Wollert, G.P. Meyer, J. Lotz, S. Ringes-Lichtenberg, P. Lippolt, C. Breidenbach, S. Fichtner, T. Korte, B. Hornig, D. Messinger, L. Arseniev, B. Hertenstein, A. Ganser, H. Drexler, Intracoronary autologous bone-marrow cell transfer after myocardial infarction: the BOOST randomised controlled clinical trial, Lancet 364 (2004) 141–148.
[7] O. Agbulut, S. Vandervelde, N. Al Attar, J. Larghero, S. Ghostine, B. Leobon, E. Robidel, P. Borsani, M. Le Lorc'h, A. Bissery, C. Chomienne, P. Bruneval, J.P. Marolleau, J.T. Vilquin, A. Hagege, J.L. Samuel, P. Menasche, Comparison of human skeletal myoblasts and bone marrow-derived CD133+ progenitors for the repair of infarcted myocardium, J. Am. Coll. Cardiol. 44 (2004) 458–463.
[8] P. Menasche, A.A. Hagege, M. Scorsin, B. Pouzet, M. Desnos, D. Duboc, K. Schwartz, J.T. Vilquin, J.P. Marolleau, Myoblast transplantation for heart failure, Lancet 357 (2001) 279–280.
[9] D.J. Prockop, Stem cell research has only just begun, Science 293 (2001) 211–212.
[10] K. Le Blanc, C. Gotherstrom, O. Ringden, M. Hassan, R. McMahon, E. Horwitz, G. Anneren, O. Axelsson, J. Nunn, U. Ewald, S. Norden-Lindeberg, M. Jansson, A. Dalton, E. Astrom, M. Westgren, Fetal mesenchymal stem-cell engraftment in bone after in utero transplantation in a patient with severe osteogenesis imperfecta, Transplantation 79 (2005) 1607–1614.
[11] K. Le Blanc, I. Rasmusson, C. Gotherstrom, C. Seidel, B. Sundberg, M. Sundin, K. Rosendahl, C. Tammik, O. Ringden, Mesenchymal stem cells inhibit the expression of CD25 (interleukin-2 receptor) and CD38 on phytohaemagglutinin-activated lymphocytes, Scand. J. Immunol. 60 (2004) 307–315.
[12] S. Makino, K. Fukuda, S. Miyoshi, F. Konishi, H. Kodama, J. Pan, M. Sano, T. Takahashi, S. Hori, H. Abe, J. Hata, A. Umezawa, S. Ogawa, Cardiomyocytes can be generated from marrow stromal cells in vitro, J. Clin. Invest. 103 (1999) 697–705.
[13] Y. Takeda, T. Mori, H. Imabayashi, T. Kiyono, S. Gojo, S. Miyoshi, N. Hida, M. Ita, K. Segawa, S. Ogawa, M. Sakamoto, S. Nakamura, A. Umezawa, Can the life span of human marrow stromal cells be prolonged by bmi-1, E6, E7, and/or telomerase without affecting cardiomyogenic differentiation? J. Gene Med. 6 (2004) 833–845.
[14] D. Orlic, J. Kajstura, S. Chimenti, I. Jakoniuk, S.M. Anderson, B. Li, J. Pickel, R. McKay, B. Nadal-Ginard, D.M. Bodine, A. Leri, P. Anversa, Bone marrow cells regenerate infarcted myocardium, Nature 410 (2001) 701–705.
[15] S. Gojo, N. Gojo, Y. Takeda, T. Mori, H. Abe, S. Kyo, J. Hata, A. Umezawa, In vivo cardiovasculogenesis by direct injection of isolated adult mesenchymal stem cells, Exp. Cell Res. 288 (2003) 51–59.
[16] J.S. Wang, D. Shum-Tim, J. Galipeau, E. Chedrawy, N. Eliopoulos, R.C. Chiu, Marrow stromal cells for cellular cardiomyoplasty: feasibility and potential clinical advantages, J. Thorac. Cardiovasc. Surg. 120 (2000) 999–1005.
[17] J.G. Shake, P.J. Gruber, W.A. Baumgartner, G. Senechal, J. Meyers, J.M. Redmond, M.F. Pittenger, B.J. Martin, Mesenchymal stem cell implantation in a swine myocardial infarct model: engraftment and functional effects, Ann. Thorac. Surg. 73 (2002) 1919–1925 (discussion 1926).
[18] K.L. Moore, T.V.N. Persaud, The Developing Human: Clinically Oriented Embryology, Saunders, Philadelphia, Pa., 2003.
[19] K. Igura, X. Zhang, K. Takahashi, A. Mitsuru, S. Yamaguchi, T.A. Takashi, Isolation and characterization of mesenchymal progenitor cells from chorionic villi of human placenta, Cytotherapy 6 (2004) 543–553.
[20] X. Zhang, A. Mitsuru, K. Igura, K. Takahashi, S. Ichinose, S. Yamaguchi, T.A. Takahashi, Mesenchymal progenitor cells derived from chorionic villi of human placenta for cartilage tissue engineering, Biochem. Biophys. Res. Commun. 340 (2006) 944–952.
[21] J. Paquin, B.A. Danalache, M. Jankowski, S.M. McCann, J. Gutkowska, Oxytocin induces differentiation of P19 embryonic stem cells to cardiomyocytes, Proc. Natl. Acad. Sci. U. S. A. 99 (2002) 9550–9555.
[22] M. Terai, T. Uyama, T. Sugiki, X.K. Li, A. Umezawa, T. Kiyono, Immortalization of human fetal cells: the life span of umbilical cord blood-derived cells can be prolonged without manipulating p16INK4a/RB braking pathway, Mol. Biol. Cell 16 (2005) 1491–1499.
[23] D.J. Prockop, I. Sekiya, D.C. Colter, Isolation and characterization of rapidly self-renewing stem cells from cultures of human marrow stromal cells, Cytotherapy 3 (2001) 393–396.
[24] I. Potapova, A. Plotnikov, Z. Lu, P. Danilo Jr., V. Valiunas, J. Qu, S. Doronin, J. Zuckerman, I.N. Shlapakova, J. Gao, Z. Pan, A.J. Herron, R.B. Robinson, P.R. Brink, M.R. Rosen, I.S. Cohen, Human mesenchymal stem cells as a gene delivery system to create cardiac pacemakers, Circ. Res. 94 (2004) 952–959.
[25] C. Badorff, R.P. Brandes, R. Popp, S. Rupp, C. Urbich, A. Aicher, I. Fleming, R. Busse, A.M. Zeiher, S. Dimmeler, Transdifferentiation of blood-derived human adult endothelial progenitor cells into functionally active cardiomyocytes, Circulation 107 (2003) 1024–1032.
[26] K. Matsuura, H. Wada, T. Nagai, Y. Iijima, T. Minamino, M. Sano, H. Akazawa, J.D. Molkentin, H. Kasanuki, I. Komuro, Cardiomyocytes fuse with surrounding noncardiomyocytes and reenter the cell cycle, J. Cell Biol. 167 (2004) 351–363.
[27] C.H. Cui, T. Uyama, K. Miyado, M. Terai, S. Kyo, T. Kiyono, A. Umezawa, Menstrual blood-derived cells confer human dystrophin expression in the murine model of duchenne muscular dystrophy via cell fusion and myogenic transdifferentiation, Mol. Biol. Cell 18 (2007) 1586–1594.
[28] T. Mori, T. Kiyono, H. Imabayashi, Y. Takeda, K. Tsuchiya, S. Miyoshi, H. Makino, K. Matsumoto, H. Saito, S. Ogawa, M. Sakamoto, J. Hata, A. Umezawa, Combination of hTERT and bmi-1, E6, or E7 induces prolongation of the life span of bone marrow stromal cells from an elderly donor without affecting their neurogenic potential, Mol. Cell. Biol. 25 (2005) 5183–5195.
[29] J. Kohyama, H. Abe, T. Shimazaki, A. Koizumi, K. Nakashima, S. Gojo, T. Taga, H. Okano, J. Hata, A. Umezawa, Brain from bone: efficient "meta-differentiation" of marrow stroma-derived mature osteoblasts to neurons with Noggin or a demethylating agent, Differentiation 68 (2001) 235–244.
[30] K.D. Lee, T.K. Kuo, J. Whang-Peng, Y.F. Chung, C.T. Lin, S.H. Chou, J.R. Chen, Y.P. Chen, O.K. Lee, In vitro hepatic differentiation of human mesenchymal stem cells Hepatology 40 (2004) 1275–1284.
[31] I. Komuro, S. Izumo, Csx: a murine homeobox-containing gene specifically expressed in the developing heart, Proc. Natl. Acad. Sci. U. S. A. 90 (1993) 8145–8149.
[32] I. Shiojima, I. Komuro, T. Mizuno, R. Aikawa, H. Akazawa, T. Oka, T. Yamazaki, Y. Yazaki, Molecular cloning and characterization of human cardiac homeobox gene CSX1, Circ. Res. 79 (1996) 920–929.
[33] Y. Yamada, K. Sakurada, Y. Takeda, S. Gojo, A. Umezawa, Single-cell-derived mesenchymal stem cells overexpressing Csx/Nkx2.5 and GATA4 undergo the stochastic cardiomyogenic fate and behave like transient amplifying cells, Exp. Cell Res. 313 (2007) 698–706.
[34] F. Ishikawa, Cellular senescence, an unpopular yet trustworthy tumor suppressor mechanism, Cancer Sci. 94 (2003) 944–947.

臨床研究

# Ross手術後の中期遠隔期の心機能
## —機械弁置換術との比較

Midterm cardiopulmonary profile of Ross procedure－Comparison with mechanical valve replacement

成田純任[1)]　石川司朗[1)]　石川友一[1)]　中村　真[1)]　牛ノ濱大也[1)]
佐川浩一[1)]　總崎直樹[2)]　中野俊秀[3)]　角　秀秋[3)]

1) 福岡市立こども病院・感染症センター循環器科，2) 同　新生児循環器科，3) 同　心臓血管外科

〈Abstract〉

**背景**：大動脈弁疾患の治療成績は人工弁の改善およびRoss手術の導入により改善してきた．手術侵襲が大きいRoss手術については特に小児において第1選択とする積極派と慎重派に見解が分かれる．

**目的**：小児期—青年期症例におけるRoss手術の中期遠隔期心機能を機械弁置換法との比較で明らかにする．

**対象**：当院が経験したRoss手術19例(Ross群：7.3～23.7歳：中央値13.4歳)と機械弁置換法18例(MV群：5.3～15.5歳：中央値12.5歳)．

**方法**：両群の上行大動脈血流速度(ascending aorta flow velocity；Ao FV)，トレッドミル運動負荷時のpeak $\dot{V}O_2$(年齢・性をマッチさせた%Normal)および内科管理の実態を術後早期から5年で比較し，Ross群はautograftの閉鎖不全，主肺動脈血流速度，肺動脈弁閉鎖不全(pulmonary regurgitation；PR)も評価した．

**結果**：データは平均値(術後期間)で表し，Ross群：MV群の順で示す．Ao FVは102±26：140±44cm/s(術後早期)，102±48：224±56cm/s(術後5年)で有意にRoss群において低く，MV群で経年的に上昇する．peak $\dot{V}O_2$(%Normal)は97.0±17.1：85±22.6%(術後3年)，97.5±26.5：83.5±16.5%(術後5年)で統計学的有意差なし．遠隔期Ross群のautograft閉鎖不全は1例を除き1度以下であり，PRもすべて1度以下であった．1例でPTFEグラフトによる肺動脈弁の石灰化のため再手術を要した．現時点でRoss群の95%は無投薬で，MV群は全例で抗凝固療法が，39%で抗心不全薬の内服が行われていた．

**結論**：大動脈弁疾患に対するRoss手術は血行動態上機械弁置換に劣らず，症例によっては第1選択となり得る．今後も半月弁機能を中心とした長期的観察が望まれる．

Sumito Narita[1)], Shiro Ishikawa[1)], Yu-ichi Ishikawa[1)], Makoto Nakamura[1)], Hiroya Ushinohama[1)], Ko-ichi Sagawa[1)], Naoki Fusazaki[2)], Toshihide Nakano[3)], Hideaki Kado[3)]

1) Department of Pediatric Cardiology, Fukuoka Children's Hospital, 2) Department of Neonatal Cardiology, Fukuoka Children's Hospital, 3) Department of Cadiovascular Surgery, Fukuoka Children's Hospital

Key words
- 大動脈弁狭窄
- 大動脈弁閉鎖不全
- Ross手術
- 大動脈弁置換術

(2006.12.4 原稿受領；2007.7.19 採用)

## はじめに

大動脈弁疾患は先天性心疾患のなかでも比較的頻度が高く約5%をしめ，しばしば大動脈弁置換術(aortic valve replacement；AVR)を要する．大動脈弁狭窄(aortic stenosis；AS)，大動脈弁閉鎖不全(aortic regurgitation；AR)に代表される大動脈弁疾患の治療成績はASへのカテーテルによるバルーン弁

**表1 患者背景**

| Operation | n | Diagnosis | | | Age (medium) | Other anomaly |
|---|---|---|---|---|---|---|
| | | AS | ASR | AR | | |
| Ross群 | 19 | 6 | 11 | 2 | 13.4歳 | CoA/VSD 1 |
| MV群 | 18 | 6 | 6 | 6 | 12.5歳 | DCRV/VSD 1 |

形成術，Ross手術の導入，人工弁のクオリティ向上により大きく改善してきた．自己肺動脈弁グラフトを使用するAVRであるRoss手術は1967年にRossらにより報告された[1]．Ross手術は成長が期待できず，永年の抗凝固療法が必要である機械弁の欠点を補完する可能性のある治療として1990年代に急速に普及し，成人および小児領域において満足できる中期成績が複数報告されている[2)~6)]．しかし本手術は大動脈弁，肺動脈弁の2弁置換であり，機械弁置換によるAVRに比し手術侵襲が大きい本法は術後の両半月弁機能不全に注意を要し，長期成績は不明である．

## ○ 目的

小児期－青年期症例におけるRoss手術の中期遠隔期心機能を機械弁置換法との比較で明らかにし，その有用性と問題点を検討すること．

## ○ 対象

当院が経験したRoss手術(Ross-Konno手術は除く)19例(1998～2005年，7.3～23.7歳：中央値13.4歳)と機械弁置換法(mechanical valve replacement群；MV群)18例(1991～1998年，5.3～15.5歳：中央値12.5歳)．症例の背景を**表1**に，症例の経過を**図1**に示す．

対象大動脈弁疾患はRoss群ではAS 6例，ASR 11例，AR 2例であり，MV群ではAS 6例，ASR 6例，AR 6例であった．合併奇形としてはRoss群で大動脈縮窄・心室中隔欠損を1例に，MV群で右室二腔症・心室中隔欠損を1例に認めた．

ASにおける手術適応の原則は安静時収縮期圧較差>50mmHgが基準であり，ASに関連した症状の発現(失神，胸痛，心不全)を認めるものとした．無症状であっても安静時あるいは中等度運動時の心電図変化があるもの，圧較差75mmHg以上では手術適応とした．ARにおいては3度以上の症例で，進行性の心不全症状，心拡大を認めるものとした．Ross手術の適応においては自己肺動脈弁の変性がないことが前提条件である．

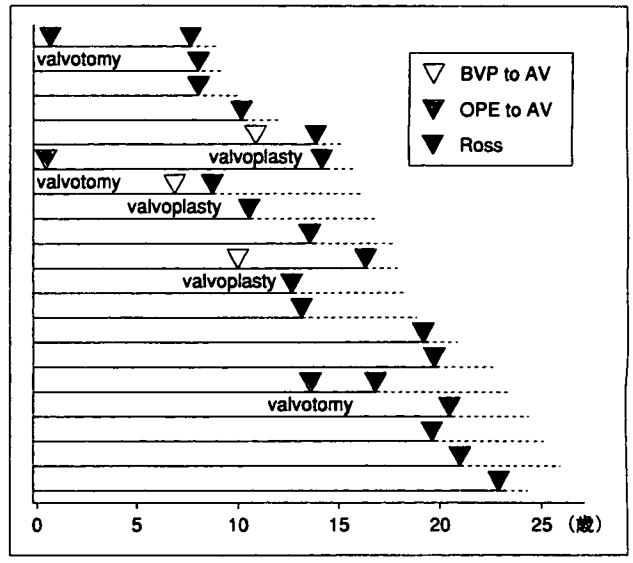

**図1 Ross症例の経過**

Ross手術における肺動脈弁再建では既製品使用が3例(Hemashield 2例，Freestyle 1例)，手縫い3弁付PTFEグラフト(井本弁)を8例，井本弁にBulging sinusを設けた山岸弁[2)]を8例で使用した．

MV群ではNicks 9例，AVR 4例，Konno 2例，Konno+Nicks 2例，modified Konno 1例であった．いずれにおいてもSt Jude Medical社製機械弁を使用した．

## ○ 方法

両群の上行大動脈血流速度(ascending aorta flow velocity；Ao FV)，トレッドミル運動負荷時の最大酸素摂取量(peak $\dot{V}O_2$：%Normal)，および内科管理の実態を術後早期(1カ月以内)から5年で経年的に比較した．Ross群においてはAR，主肺動脈血流速度，肺動脈弁閉鎖不全(pulmonary regurgitation；PR)も評価した．血流速度計測は心エコー(SONOS